J|A|C|S
ARTICLES
Published on Web 09/16/2004

Molybdenocene Trihydride Complexes: Influence of a [Me_2Si] *Ansa* Bridge on Classical versus Nonclassical Nature, Stability with Respect to Elimination of Dihydrogen, and Acidity

Kevin E. Janak, Jun Ho Shin, and Gerard Parkin*

Contribution from the Department of Chemistry, Columbia University, New York, New York 10027

Received April 27, 2004; E-mail: parkin@chem.columbia.edu

Abstract: Experimental and computational studies on a series of cationic molybdenocene trihydride complexes, namely $[Cp_2MoH_3]^+$, $[(Cp^{But})_2MoH_3]^+$, $[Cp^*_2MoH_3]^+$, and $\{[Me_2Si(C_5Me_4)_2]MoH_3\}^+$, demonstrate that the most stable form for the *ansa* molybdenocene derivative is a nonclassical dihydrogen−hydride isomer, $\{[Me_2Si(C_5Me_4)_2]Mo(\eta^2\text{-}H_2)(H)\}^+$, whereas the stable forms for the non-*ansa* complexes are classical trihydrides, $[Cp_2Mo(H)_3]^+$, $[(Cp^{But})_2Mo(H)_3]^+$, and $[Cp^*_2Mo(H)_3]^+$. In addition to altering the classical versus nonclassical nature of $[Cp^*_2MoH_3]^+$ and $\{[Me_2Si(C_5Me_4)_2]Mo(\eta^2\text{-}H_2)(H)\}^+$, the [$Me_2Si$] *ansa* bridge also markedly influences the stability of the complex with respect to elimination of H_2 and dissociation of H^+. Finally, computational studies on $\{[H_2Si(C_5H_4)_2]MoH_2D\}^+$ and $\{[H_2Si(C_5H_4)_2]MoHD_2\}^+$ establish that deuterium exhibits a greater preference than hydrogen to occupy dihydrogen versus hydride sites.

Introduction

Transition metal hydride complexes $[MH_x]$ exhibit a wide range of reactivity and play important roles in catalysis and metal-mediated transformations.[1] However, in view of the seminal discovery by Kubas of the existence of dihydrogen complexes $[M(\eta^2\text{-}H_2)]$,[2,3] it is now recognized that a complete understanding of the reactivity of metal−"hydride"[4] systems requires knowledge pertaining to both classical metal−hydride $[M(H)_x]$ and nonclassical metal−dihydrogen $[M(\eta^2\text{-}H_2)]$ ligands. It is, therefore, important to understand the factors that influence the kinetics and thermodynamics of the interconversion of isomeric classical hydride and nonclassical dihydrogen complexes and also the reactivity of these isomers. In this paper, we describe the influence of cyclopentadienyl substituents on the equilibrium between dihydrogen−hydride and trihydride complexes in the molybdenocene system.

Molybdenocene and tungstenocene dihydride complexes $(Cp^R)_2MH_2$[5] have long played a prominent role in the development of organometallic chemistry, and it is well known that the d^2 metal centers of these complexes may be readily protonated to give "trihydride" derivatives $[(Cp^R)_2MH_3]^+$.[6] Of particular interest, however, is the issue of whether the $[(Cp^R)_2MH_3]^+$ cations are formally characterized as classical trihydride $[MH_3]$ or nonclassical dihydrogen−hydride $[M(\eta^2\text{-}H_2)H]$ complexes and whether the equilibrium between these isomers is facile (Scheme 1).[7]

The most useful means of differentiating between classical and nonclassical hydride tautomers in solution is often provided by ^{1}H NMR spectroscopy. For example, the hydride ligands of both $[Cp_2WH_3]^+$ ($^2J_{HH}$ = 8.5 Hz)[6,8] and $[Cp^*_2WH_3]^+$ ($^2J_{HH}$ = 3 Hz)[9] are characterized by a pair of doublet and triplet sets of resonances, with small values of the $^2J_{HH}$ coupling constants that are indicative of a trihydride formulation.[10] However,

(1) (a) Hoskin, A. J.; Stephan, D. W. *Coord. Chem. Rev.* **2002**, *233*−*234*, 107−129. (b) McGrady, G. S.; Guilera, G. *Chem. Soc. Rev.* **2003**, *32*, 383−392. (c) Hlatky, H.; Crabtree, R. H. *Coord. Chem. Rev.* **1985**, *65*, 1−48. (d) Kuhlman, R. *Coord. Chem. Rev.* **1997**, *167*, 205−232. (e) Esteruelas, M. A.; Oro, L. A. *Chem. Rev.* **1998**, *98*, 577−588. (f) Gusev, D. G.; Berke, H. *Chem. Ber*. **1996**, *129*, 1143−1155.

(2) Kubas, G. J.; Ryan, R. R.; Swanson, B. I.; Vergamini, P. J.; Wasserman, J. J. *J. Am. Chem. Soc.* **1984**, *106*, 451−452.

(3) (a) Kubas, G. J. *Metal Dihydrogen and σ-Bond Complexes: Structure, Theory, and Reactivity*; Kluwer Academic/Plenum Publishers: New York, 2001. (b) Kubas, G. J. *J. Organomet. Chem.* **2001**, *635*, 37−68. (c) Heinekey, D. M.; Oldham, W. J. *Chem. Rev.* **1993**, *93*, 913−926. (d) Jessop, P. G.; Morris, R. H. *Coord. Chem. Rev.* **1992**, *121*, 155−284. (e) Lin, Z.; Hall, M. B. *Coord. Chem. Rev.* **1994**, *135/136*, 845−879. (f) Crabtree, R. H. *Acc. Chem. Res.* **1990**, *23*, 95−101.

(4) The word "hydride" when used in quotes, and the abbreviation H_n, are used to encompass both classical and nonclassical hydride ligands where no distinction is intended. When a distinction is intended, the hydrogen atoms are placed in parentheses, with classical hydride ligands being represented by $(H)_n$, and nonclassical dihydrogen ligands being represented by $(\eta^2\text{-}H_2)$.

(5) The abbreviation Cp^R is used to indicate any cyclopentadienyl ligand, regardless of the nature and number of the ring substituents.

(6) Green, M. L. H.; McLeverty, J. A.; Pratt, L.; Wilkinson, G. *J. Chem. Soc. A* **1961**, 4854−4859.

(7) For example, $[CpIr(PMe_3)H_3]^+$,[a] $[Cp^*Ir(PMe_3)H_3]^+$,[b] and $CpRu(PCy_3)H_3$[c] exist as classical trihydrides, whereas $[Cp^*Rh(PMe_3)(\eta^2\text{-}H_2)(H)]^+$,[d] $\{[Tp]Ir(PMe_3)(\eta^2\text{-}H_2)(H)\}^+$,[e,f] and $[Tp^{Me_2}]Ru(PMe_3)(\eta^2\text{-}H_2)(H)$[g] are nonclassical dihydrogen−hydride complexes. (a) Heinekey, D. M.; Millar, J. M.; Koetzle, T. F.; Payne, N. G.; Zilm, K. W. *J. Am. Chem. Soc.* **1990**, *112*, 909−919. (b) Heinekey, D. M.; Hinkle, A. S.; Close, J. D. *J. Am. Chem. Soc.* **1996**, *118*, 5353−5361. (c) Arliguie, T.; Chaudret, B. *J. Chem. Soc., Chem. Commun.* **1986**, 985−986. (d) Taw, F. L.; Mellows, H.; White, P. S.; Hollander, F. J.; Bergman, R. G.; Brookhart, M.; Heinekey, D. M. *J. Am. Chem. Soc.* **2002**, *124*, 5100−5108. (e) Heinekey, D. M.; Oldham, W. J. *J. Am. Chem. Soc.* **1994**, *116*, 3137−3138. (f) Oldham, W. J.; Hinkle, A. S.; Heinekey, D. M. *J. Am. Chem. Soc.* **1997**, *119*, 11028−11036. (g) Moreno, B.; Sabo-Etienne, S.; Chaudret, B.; Rodriguez, A.; Jalon, F.; Trofimenko, S. *J. Am. Chem. Soc.* **1995**, *117*, 7441−7451.

(8) Heinekey, D. M. *J. Am. Chem. Soc.* **1991**, *113*, 6074−6077.

(9) (a) Parkin, G.; Bercaw, J. E. *Polyhedron* **1988**, *7*, 2053−2082. (b) Parkin, G.; Bercaw, J. E. *J. Chem. Soc., Chem. Commun.* **1989**, 255−257.

10.1021/ja047554c CCC: $27.50

Scheme 1

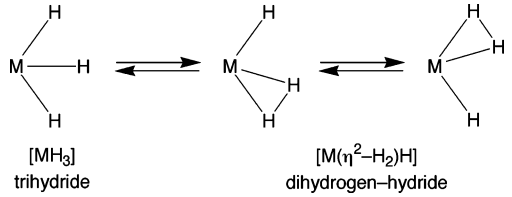

consideration of the parent molybdenocene complex, $[Cp_2MoH_3]^+$, indicates that the use of ^{1}H NMR spectroscopy to distinguish between classical and nonclassical formulations is not necessarily straightforward. Thus, rather than feature the simple doublet and triplet pattern exhibited by $[Cp_2WH_3]^+$, the ^{1}H NMR spectrum of the molybdenum counterpart $[Cp_2MoH_3]^+$ is characterized by a *singlet* in the hydride region at room temperature.[6] The form of the spectrum, however, is very temperature dependent, and Heinekey has demonstrated that upon cooling to −70 °C a highly second-order static AB_2 spectrum is obtained, with $^2J_{HH(min)} \approx 1000$ Hz.[8] The observation of a singlet at room temperature was rationalized in terms of facile hydride exchange between the central and lateral sites, while the large coupling constant at low temperature was attributed to quantum mechanical exchange, a mechanism by which $^2J_{HH}$ may be increased significantly from that of the traditional magnetic scalar coupling,[11−14] with $J_{obs} = J_m - 2J_{ex}$.[12c] As such, an observed J_{HH} coupling constant comparable to that in H_2 does not, per se, indicate that a compound is a nonclassical hydride.

Quantum mechanical exchange coupling is not restricted to molybdenocene complexes, and has also been observed for tungstenocene trihydride derivatives with *ansa* bridges, namely $\{[Me_2Si(C_5H_4)_2]WH_3\}^+$ and $\{[Me_2C(C_5H_4)_2]WH_3\}^+$.[15] For example, $^2J_{HH}$ for $\{[Me_2Si(C_5H_4)_2]WH_3\}^+$ varies from 8 Hz at −140 °C to 75 Hz at 0 °C, while $^2J_{HH}$ for $\{[Me_2C(C_5H_4)_2]WH_3\}^+$ varies from 2900 Hz at −130 °C to 16 000 Hz at −70 °C. Calculations on these *ansa* tungstenocene derivatives with large coupling constants, nevertheless, indicate that they possess classical trihydride structures.[14] Notwithstanding the fact that a variety of $[Cp^R_2WH_3]^+$ derivatives exist as classical trihydrides, evidence has been presented that nonclassical hydride complexes are involved as unstable intermediates in the formation of the trihydrides by protonation of Cp_2WH_2[16] and $Cp^*_2WH_2$.[9] Likewise, the molybdenum dihydrogen−hydride species $[Cp_2Mo(\eta^2\text{-}H_2)H]^+$ has been invoked as an intermediate in the formation of $[Cp_2MoH_3]^+$ by protonation of Cp_2MoH_2.[16] Since the steric and electronic effects of cyclopentadienyl ring substituents may have a pronounced impact on the chemistry of a system,[17] we sought to determine whether modification of these substituents could provide a sufficient perturbation to allow the dihydrogen−hydride isomer to become favored. With this aim in mind, we chose to focus attention on molybdenocene rather than tungstenocene derivatives because metals of the second transition series more commonly yield nonclassical hydride complexes than do their third transition series congeners.[3] Therefore, we report here an investigation of a series of $[(Cp^R)_2MoH_3]^+$ derivatives, namely $[(Cp^{But})_2MoH_3]^+$, $[Cp^*_2MoH_3]^+$, and $\{[Me_2Si(C_5Me_4)_2]MoH_3\}^+$, each of which is obtained by protonation of the respective dihydride $(Cp^R)_2MoH_2$.[18] In particular, comparison of $[Cp^*_2MoH_3]^+$ and $\{[Me_2Si(C_5Me_4)_2]MoH_3\}^+$ demonstrates that the $[Me_2Si]$ *ansa* bridge increases (i) the tendency of the complex to form a dihydrogen−hydride derivative, (ii) the tendency of the complex to eliminate H_2, and (iii) the acidity of the complex. The characterization of the *ansa* complex $\{[Me_2Si(C_5Me_4)_2]Mo(\eta^2\text{-}H_2)(H)\}^+$ as a dihydrogen−hydride complex is also noteworthy since dihydrogen−hydride complexes with a d^2 configuration are particularly rare.[19]

Results and Discussion

Variable-Temperature ^{1}H NMR Spectroscopic Studies of $[(Cp^R)_2MoH_3]^+$. Analogous to $[Cp_2MoH_3]^+$,[8] the hydride regions of the ^{1}H NMR spectra of $[(Cp^{But})_2MoH_3]^+$ and $[Cp^*_2MoH_3]^+$ are highly temperature dependent, as illustrated for $[Cp^*_2MoH_3]^+$ in Figure 1.[20] Specifically, the hydride ligands are characterized by a singlet at room temperature but a symmetric 1:10:1 pattern at low temperature. The 1:10:1 triplet pattern for the hydride region of $[Cp^*_2MoH_3]^+$ indicates a highly second-order AB_2 spin system for which $J_{AB} > 20\ \Delta_{AB}$.[21,22] The rather simple appearance of the hydride region of $[Cp^*_2MoH_3]^+$ at low temperature is, therefore, attributed to a very large J_{AB} coupling constant relative to the magnitude of the chemical shift difference. For AB_2 (and, *mutatis mutandis*, A_2B) spectra with sufficiently large J_{AB}/Δ_{AB} ratios that a 1:10:1 triplet pattern is observed, (i) the intense central resonance corresponds to the weighted average of the A and B chemical shifts, i.e. $\delta_{av} = [(\delta_A + 2\delta_B)/3]$, and (ii) the separation between the "satellite" signals is directly related to the difference in chemical shifts of the A and B sites, i.e. $\Delta_{satellite} = 1.333|(\delta_A - \delta_B)|$.[23] As a result of the highly second-order nature of the AB_2 pattern, it is only possible to determine a minimum value for J_{HH} (Table 1); nevertheless, it is evident that these coupling constants are sufficiently large to be indicative of a quantum mechanical exchange mechanism. In accord with a quantum mechanical exchange mechanism, the observed coupling constants are also

(10) $^2J_{HH}$ values are typically in the range 2−18 Hz. See, for example, ref 7b and ref 37 therein.
(11) (a) Jones, D. H.; Labinger, J. A.; Weitekamp, D. P. *J. Am. Chem. Soc.* **1989**, *111*, 3087−3088. (b) Bowers, C. R.; Jones, D. H.; Kurur, N. D.; Labinger, J. A.; Pravica, M. G.; Weitekamp, D. P. *Adv. Magn. Reson.* **1990**, *14*, 269−291.
(12) (a) Zilm, K. W.; Heinekey, D. M.; Millar, J. M.; Payne, N. G.; Demou, P. *J. Am. Chem. Soc.* **1989**, *111*, 3088−3089. (b) Reference 7a. (c) Zilm, K. W.; Heinekey, D. M.; Millar, J. M.; Payne, N. G.; Neshyba, S. P.; Duchamp, J. C.; Szczyrba, J. *J. Am. Chem. Soc.* **1990**, *112*, 920−929. (d) Heinekey, D. M.; Payne, N. G.; Sofield, C. D. *Organometallics* **1990**, *9*, 2643−2645.
(13) (a) Sabo-Etienne, S.; Chaudret, B. *Chem. Rev.* **1998**, *98*, 2077−2091. (b) Maseras, F.; Lledós, A.; Clot, E.; Eisenstein, O. *Chem. Rev.* **2000**, *100*, 601−636.
(14) (a) Green, J. C.; Scottow, A. *New J. Chem.* **1999**, *23*, 651−655. (b) Camanyes, S.; Maseras, F.; Moreno, M.; Lledós, A.; Lluch, J. M.; Bertrán, J. *J. Am. Chem. Soc.* **1996**, *118*, 4617−4621.
(15) (a) Chernega, A.; Cook, J.; Green, M. L. H.; Labella, L.; Simpson, S. J.; Souter, J.; Stephens, A. H. H. *J. Chem. Soc., Dalton Trans.* **1997**, 3225−3243. (b) Conway, S. L. J.; Dijkstra, T.; Doerrer, L. H.; Green, J. C.; Green, M. L. H.; Stephens, A. H. H. *J. Chem. Soc., Dalton Trans.* **1998**, 2689−2695.
(16) Henderson, R. A.; Oglieve, K. E. *J. Chem. Soc., Dalton Trans.* **1993**, 3431−3439.
(17) Zachmanoglou, C. E.; Docrat, A.; Bridgewater, B. M.; Parkin, G.; Brandow, C. G.; Bercaw, J. E.; Jardine, C. N.; Lyall, M.; Green, J. C.; Keister, J. B. *J. Am. Chem. Soc.* **2002**, *124*, 9525−9546.
(18) For the syntheses of $(Cp^{But})_2MoH_2$,[a] $Cp^*_2MoH_2$,[b] and $[Me_2Si(C_5Me_4)_2]MoH_2$,[c] see: (a) Shin, J. H.; Savage, W.; Murphy, V. J.; Bonanno, J. B.; Churchill, D. G.; Parkin, G. *J. Chem. Soc., Dalton Trans.* **2001**, 1732−1753. (b) Thomas, J. L. *J. Am. Chem. Soc.* **1973**, *95*, 1838−1848. (c) Churchill, D.; Shin, J. H.; Hascall, T.; Hahn, J. M.; Bridgewater, B. M.; Parkin, G. *Organometallics* **1999**, *18*, 2403−2406.
(19) Pons, V.; Conway, S. L. J.; Green, M. L. H.; Green, J. C.; Herbert, B. J.; Heinekey, D. M. *Inorg. Chem.* **2004**, *43*, 3475−3483 and references therein.
(20) It is also pertinent to note that the appearance of the spectrum is solvent dependent. See ref 8.
(21) Bovey, F. A.; Jelinski, L.; Mirau, P. A. *Nuclear Magnetic Resonance*, 2nd ed.; Academic Press: New York, 1988.
(22) See Supporting Information.

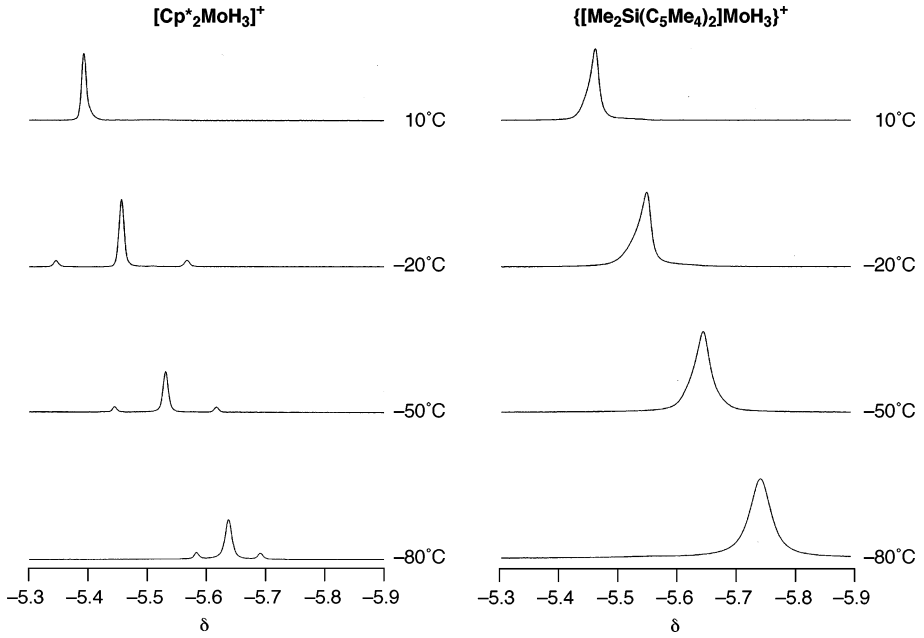

Figure 1. Variable-temperature ^{1}H NMR spectra (500 MHz) of the hydride regions of $[Cp^*_2MoH_3]^+$ and $\{[Me_2Si(C_5Me_4)_2]Mo(\eta^2\text{-}H_2)(H)\}^+$.

Table 1. Minimum J_{HH} Coupling Constants for $[(Cp^R)_2MoH_3]^+$ Derivatives

$[Cp_2MoH_3]^+$		$[Cp^*_2MoH_3]^+$		$[(Cp^{But})_2MoH_3]^+$	
T/°C	$J_{HH(min)}$/Hz	T/°C	$J_{HH(min)}$/Hz	T/°C	$J_{HH(min)}$/Hz
−80	375	−80	100	−80	530
−70	465	−70	125	−70	570
−60	550	−60	173	−60	605
−50	625	−50	230	−50	625
−40	710	−40	305	−40	690
−30	800	−30	370	−30	770
−20	925	−20	425	−20	900
		−10	470	−10	1100
		0	600		
		10	800		

highly temperature dependent (Table 1).[11−13] Since the observed J_{HH} coupling constants are influenced by quantum mechanical exchange, the data are incapable of providing a definitive statement regarding the classical versus nonclassical nature of the complexes. T_1 relaxation studies (as discussed in more detail below), however, indicate that the non-*ansa* complexes $[Cp_2MoH_3]^+$, $[(Cp^{But})_2MoH_3]^+$, and $[Cp^*_2MoH_3]^+$ are appropriately characterized as classical hydride complexes.

In addition to decoalescing into a 1:10:1 AB_2 triplet, the chemical shifts of the three signals shift to higher field as the temperature is lowered (Figure 1). The chemical shift difference between the two satellites also decreases, thereby indicating that the chemical shifts of the central and lateral sites do not have the same temperature dependence, with the difference becoming smaller as the temperature is lowered.[22]

Also noteworthy is that the satellites of the static 1:10:1 AB_2 triplet broaden as the temperature is raised (Figure 1). The broadening of these satellites is a result of thermally induced chemical exchange between the central and lateral sites, as illustrated in Figure 2. Simulation of the AB_2 spectra allow the rate of chemical exchange between the central and lateral sites to be determined for $[Cp_2MoH_3]^+$, $[(Cp^{But})_2MoH_3]^+$, and $[Cp^*_2MoH_3]^+$ (Table 2). Comparison of the activation parameters indicates that the barrier to central/lateral site exchange increases in the sequence $[Cp_2MoH_3]^+ < [(Cp^{But})_2MoH_3]^+ < [Cp^*_2MoH_3]^+$, a trend that may be readily rationalized in terms of (i) increased steric interactions between the hydride ligands and ring substituents preventing the out-of-plane displacement of the hydride ligands that is required to achieve the central/lateral site exchange, and (ii) the accessibility of a dihydrogen−hydride intermediate being less favored for the more electron-donating substituents.[24]

Ansa bridges have been shown to induce interesting differences in the chemistry of molybdenocene and tungstenocene systems.[15,18c,25] We are particularly interested in the *ansa* effect as it pertains to permethylated metallocene systems[26] and therefore sought to investigate $\{[Me_2Si(C_5Me_4)_2]MoH_3\}^+$ for comparison with $[Cp^*_2MoH_3]^+$. Significantly, the spectroscopic properties of $\{[Me_2Si(C_5Me_4)_2]MoH_3\}^+$ proved to be quite distinct from those of $[Cp^*_2MoH_3]^+$.[27] For example, in contrast to the 1:10:1 AB_2 triplets that are observed for the non-*ansa* derivatives, $[Cp_2MoH_3]^+$, $[(Cp^{But})_2MoH_3]^+$, and $[Cp^*_2MoH_3]^+$, the hydride ligands of the *ansa* molybdenocene complex

(23) In view of the fact that only the modulus of $|(\delta_A - \delta_B)|$ is known, it is not possible to determine uniquely δ_A and δ_B from the observed values of δ_{av} and $\Delta_{satellite}$. Specifically, two solutions are possible in which the chemical shift of the unique central hydride ligand corresponds to either the low-field satellite or the high-field satellite; these solutions relate to whether the spin system is classified as AB_2 or A_2B, i.e. whether the chemical shift of the central hydride ligand is downfield (AB_2) or upfield (A_2B) from those of the lateral hydride ligands. For example, the hydride region of $[Cp^*_2MoH_3]^+$ at −70 °C may be simulated as either an AB_2 spectrum with $\delta_A = -5.533$ and $\delta_B = -5.630$ ($J_{AB} \geq 125$ Hz), or as an A_2B spectrum with $\delta_A = -5.565$ and $\delta_B = -5.663$ ($J_{AB} \geq 125$ Hz). On the basis of studies on the $[Cp^*_2MoHD_2]^+$ isotopologue, however, it is evident that the correct solution is AB_2 in which the chemical shift of the central hydride ligand is at lower field than that of the lateral hydride ligands (specifically, the $[Cp^*_2MoHD_2]^+$ isotopologue is characterized by two signals in the ratio 2:1 for the isotopomers with H in the lateral and central positions, respectively). See Supporting Information.

(24) Calculations on $[(Cp^R)_2WH_3]^+$ derivatives indicate that the central/lateral site exchange involves a transition state which features a dihydrogen ligand that is perpendicular to the metallocene plane. See ref 14a.

(25) (a) Labella, L.; Chernega, A.; Green, M. L. H. *J. Chem. Soc., Dalton Trans.* **1995**, 395−402. (b) Churchill, D. G.; Bridgewater, B. M.; Parkin, G. *J. Am. Chem. Soc.* **2000**, *122*, 178−179. (c) Churchill, D. G.; Janak, K. E.; Wittenberg, J. S.; Parkin, G. *J. Am. Chem. Soc.* **2003**, *125*, 1403−1420.

(26) See, for example: (a) Lee, H.; Desrosiers, P. J.; Guzei, I.; Rheingold, A. L.; Parkin, G. *J. Am. Chem. Soc.* **1998**, *120*, 3255−3256. (b) Reference 18c. (c) References 25b,c.

Table 2. Rate Constants for Central-to-Lateral Hydride Ligand Site Exchange for $[(Cp^R)_2MoH_3]^+$ Derivatives

$[Cp_2MoH_3]^+$		$[(Cp^{But})_2MoH_3]^+$		$[Cp^*_2MoH_3]^+$		$\{[Me_2Si(C_5Me_4)_2]Mo(\eta^2-H_2)(H)\}^+$ [a]	
T/°C	*k*/s^{-1}	*T*/°C	*k*/s^{-1}	*T*/°C	*k*/s^{-1}	*T*/°C	*k*/s^{-1}
−60	3	−50	5	−20	2	−85	40
−50	9	−40	18	−10	5	−80	70
−40	25	−30	45	0	15	−70	320
−30	90	−20	120	10	55	−60	1200
−20	175	−10	300	25	350	−50	3000
$\Delta H^{\ddagger} = 10.7(5)$ kcal mol^{-1}		$\Delta H^{\ddagger} = 11.3(2)$ kcal mol^{-1}		$\Delta H^{\ddagger} = 17(1)$ kcal mol^{-1}		$\Delta H^{\ddagger} = 10.2(3)$ kcal mol^{-1}	
$\Delta S^{\ddagger} = -5(2)$ eu		$\Delta S^{\ddagger} = -4(1)$ eu		$\Delta S^{\ddagger} = 9(4)$ eu		$\Delta S^{\ddagger} = 4(2)$ eu	
$\Delta G^{\ddagger}_{(25°C)} = 12.2$ kcal mol^{-1}		$\Delta G^{\ddagger}_{(25°C)} = 12.5$ kcal mol^{-1}		$\Delta G^{\ddagger}_{(25°C)} = 14.3$ kcal mol^{-1}		$\Delta G^{\ddagger}_{(25°C)} = 9.0$ kcal mol^{-1}	

[a] Data for MoH_2D isotopologue.

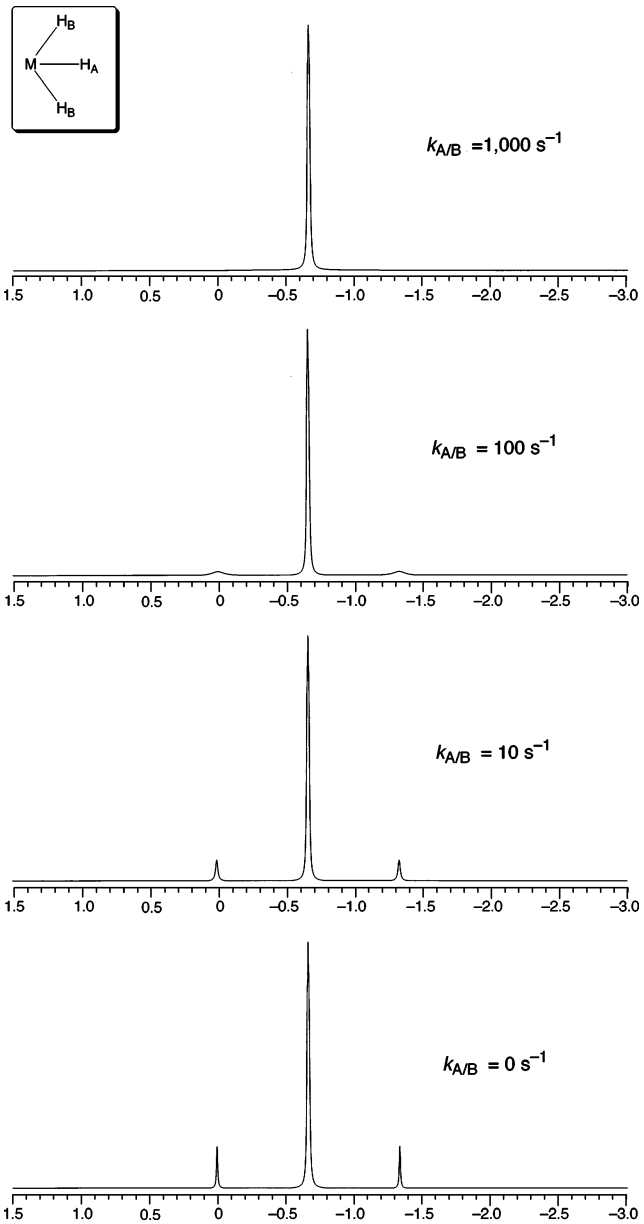

Figure 2. Influence of central (A) and lateral (B) hydride site exchange on the satellites of a 1:10:1 AB_2 triplet for which $\delta_A = 0$ ppm, $\delta_B = -1.0$ ppm, and $J_{AB} = 10\,000$ Hz.

$\{[Me_2Si(C_5Me_4)_2]MoH_3\}^+$ appear as a *singlet* over the entire temperature range of 25 to −80 °C (Figure 1).

The observation of a singlet for $\{[Me_2Si(C_5Me_4)_2]MoH_3\}^+$ at low temperature does not enable one to distinguish between a fluxional trihydride complex with a highly second-order AB_2 spin system or a fluxional dihydrogen−hydride complex with a highly second-order ABC system. In an effort to resolve this ambiguity and provide evidence for the classical versus nonclassical nature of $\{[Me_2Si(C_5Me_4)_2]MoH_3\}^+$, we performed additional experiments to determine T_1 relaxation times and J_{HD} coupling constants.

Evidence for Nonclassical Character of $\{[Me_2Si(C_5Me_4)_2]Mo(\eta^2\text{-}H_2)(H)\}^+$ Based on T_1 Relaxation Time Measurements. Measurement of the spin−lattice (longitudinal) T_1 relaxation time provides, in principle, a means to distinguish between a classical and nonclassical hydride complex because dipole−dipole relaxation, the principal relaxation mechanism for protons that are separated by less than 2 Å, is strongly distance dependent ($T_1 \propto r^6$).[28,29] However, since the relaxation rate is also influenced by molecular rotation, and hence temperature, this method is most appropriately used when dealing with the minimum value of T_1 which is independent of molecular tumbling. The temperature dependence of the T_1 values of the various $[(Cp^R)_2MoH_3]^+$ complexes has therefore been determined (Table 3). Although data at sufficiently low temperatures to determine the minimum value of T_1 for $[(Cp^R)_2MoH_3]^+$ were not obtained, comparison with the T_1 values of the respective $(Cp^R)_2MoH_2$ dihydride complexes provides a qualitative indication of T_1 variations resulting from changes involving H···H separation because the two complexes have a very similar size and hence similar rotational properties.

The T_1 values of $(Cp^R)_2MoH_2$, therefore, provide benchmarks for the relaxation times of hydride ligands in each system in the absence of a short H−H distance; for example, neutron diffraction studies on Cp_2MoH_2 definitively characterize it as a classical dihydride complex on the basis that the H···H distance is 2.06,[30,31] and the T_1 value for this molecule at −80 °C is 901 ms. Taking all dipole−dipole interactions into account,[29,32] the T_1(min) value of Cp_2MoH_2 calculated on the basis of the structure determined by neutron diffraction is 446 ms, which is

(27) In this regard Green, Green, and Heinekey have recently studied the NMR spectroscopic properties of the *ansa* complex $\{[Me_2C(C_5H_4)_2]MoH_3\}^+$ and have demonstrated that the stable isomer is the dihydrogen−hydride species $\{[Me_2C(C_5H_4)_2]Mo(\eta^2\text{-}H_2)(H)\}^+$ which exhibits hindered rotation of the dihydrogen ligand. See ref 19.

(28) (a) Bakhmutov, V. I.; Vorontsov, E. V. *Rev. Inorg. Chem.* **1998**, *18*, 183−221. (b) Crabtree, R. H.; Hamilton, D.; Lavin, M. *ACS Symp. Ser.* **1987**, *357*, 223−226. (c) Reference 3f.

(29) Desrosiers, P. J.; Cai, L.; Lin, Z.; Richards, R.; Halpern, J. *J. Am. Chem. Soc.* **1991**, *113*, 4173−4184.

(30) Schultz, A. J.; Stearley, K. L.; Williams, J. M.; Mink, R.; Stucky, G. D. *Inorg. Chem.* **1977**, *16*, 3303−3306.

(31) Specifically, the H−H distance in free H_2 is 0.74 Å and dihydrogen complexes are characterized by H−H distances of 0.8−0.9 Å, while classical hydride complexes are characterized by H···H distances greater than 1.6 Å; complexes with intermediate H−H separations in the range 1.0−1.4 Å have also been observed and are termed "elongated" or "stretched" dihydrogen complexes. See ref 3.

Table 3. Comparison of Calculated and Experimental T_1 Values for the Hydride Ligands of $(Cp^R)_2MoH_2$ and $[(Cp^R)_2MoH_3]^+$ Derivatives at 500 MHz

	R_{HH}/s^{-1} [a]	R_{MH}/s^{-1} [b]	R_{CpH}/s^{-1} [c]	R/s^{-1} [d]	R_{HH}/R (%)	T_1(min)/ms calc	T_1(−80 °C)/ms expt
Cp_2MoH_2	1.08	0.04	0.92	2.04	53	490	901
Cp_2MoH_2 (neutron struct)	1.01	0.04	1.20	2.24	45	446	901
$(Cp^{But})_2MoH_2$	1.18	0.04	1.08	2.30	51	435	397
$Cp^*_2MoH_2$	0.97	0.04	1.31	2.33	42	430	944
$[Me_2Si(C_5Me_4)_2]MoH_2$	1.07	0.04	0.94	2.05	52	488	620
$[Cp_2MoH_3]^+$	5.39[e]	0.04	0.84	6.27	86	159	307
$[(Cp^{But})_2MoH_3]^+$	5.20[f]	0.04	1.33	6.57	79	152	132
$[Cp^*_2MoH_3]^+$	5.37[g]	0.04	1.22	6.63	81	151	291
$[Cp^*_2Mo(H)(H_2)]^+$	74.6[h]	0.03	1.16	75.8	98	13	NA
$\{[Me_2Si(C_5Me_4)_2]Mo(H)(H_2)\}^+$	98.2[i]	0.03	0.87	99.14	99	10	33
$\{[Me_2Si(C_5Me_4)_2]Mo(H)_3\}^+$	5.74[j]	0.04	0.94	6.72	85	149	NA

[a] R_{HH} = hydride−hydride component (average values where appropriate). [b] R_{MH} = metal−hydride component (average values where appropriate). [c] R_{CpH} = Cp−hydride component (average values where appropriate). [d] R = total relaxation rate constant = $R_{HH} + R_{MH} + R_{CpH}$. [e] Individual values: 4.12 s^{-1} (both lateral) and 7.94 s^{-1} (central). [f] Individual values: 3.92 and 4.00 s^{-1} (lateral) and 7.68 s^{-1} (central). [g] Individual values: 4.07 and 4.13 s^{-1} (lateral) and 7.91 s^{-1} (central). [h] Individual values: 110.5 s^{-1} (*exo* H_2), 111.7 s^{-1} (*endo* H_2), and 1.67 s^{-1} (hydride). [i] Individual values: 146.1 s^{-1} (*exo* H_2), 147.1 s^{-1} (*endo* H_2), and 1.51 s^{-1} (hydride). [j] Individual values: 4.36 and 4.40 s^{-1} (lateral) and 8.45 s^{-1} (central).

in reasonable agreement with the experimental T_1 value at −80 °C, especially considering that the experimental value does not correspond to T_1(min).

Since the neutron diffraction structures of $(Cp^{But})_2MoH_2$, $Cp^*_2MoH_2$, and $[Me_2Si(C_5Me_4)_2]MoH_2$ are not available, we have used DFT geometry-optimized structures to provide an estimate for the T_1(min) values of these complexes. In this regard, the T_1(min) values for the geometry-optimized and experimentally determined structures of Cp_2MoH_2 are very similar, 490 and 446 ms, respectively. The calculated T_1(min) values for the other classical dihydrides $(Cp^R)_2MoH_2$ are also similar and range from 430 to 490 ms (Table 3).[33] As noted above, only upper limits for the experimental T_1(min) values are known, but these are nevertheless of a comparable magnitude (397−901 ms) to the calculated T_1(min) values.

Of most relevance is the direct comparison between the T_1 values of the dihydride complexes $(Cp^R)_2MoH_2$ and those of the respective trihydride derivatives $[(Cp^R)_2MoH_3]^+$ (Table 3), from which it is evident that the T_1 values of $[(Cp^R)_2MoH_3]^+$ are much shorter than those of the corresponding $(Cp^R)_2MoH_2$ derivative at the same temperature. The shorter T_1 value for the trihydride $[(Cp^R)_2MoH_3]^+$ is a consequence of the presence of an additional hydride ligand in the equatorial plane that necessarily causes closer H···H contacts. For example, comparison of the calculated structures of Cp_2MoH_2 and $[Cp_2MoH_3]^+$ indicates that the nonbonded H···H distance in $[Cp_2MoH_3]^+$ (1.63 Å) is significantly shorter than that in Cp_2MoH_2 (2.03 Å). Hydride−hydride dipolar relaxation (R_{HH}) therefore provides a much more significant contribution to the total relaxation for $[(Cp^R)_2MoH_3]^+$ than for $(Cp^R)_2MoH_2$, as illustrated by the ratios R_{HH}/R listed in Table 3. For example, hydride−hydride interactions provide 86% of the total relaxation for $[Cp_2MoH_3]^+$, but only 53% for Cp_2MoH_2.

Most significantly, the T_1 values for the *ansa* molybdenocene trihydride complex $\{[Me_2Si(C_5Me_4)_2]MoH_3\}^+$ are substantially shorter than the values for other $[(Cp^R)_2MoH_3]^+$ derivatives at the same temperature. For example, at −80 °C, the T_1 value of $\{[Me_2Si(C_5Me_4)_2]MoH_3\}^+$ (33 ms) is almost an order of magnitude shorter than that for $[Cp^*_2MoH_3]^+$ (291 ms). Since $\{[Me_2Si(C_5Me_4)_2]MoH_3\}^+$ and $[Cp^*_2MoH_3]^+$ have comparable sizes and rotational properties, the difference in T_1 values at the same temperature provides a qualitative indication that the "hydride" ligands in the *ansa* complex are on average substantially closer together than those in $[Cp^*_2MoH_3]^+$.

The experimentally determined T_1 values are, therefore, in accord with the notion that the *ansa* complex exists as a nonclassical dihydrogen−hydride species $\{[Me_2Si(C_5Me_4)_2]Mo(\eta^2\text{-}H_2)(H)\}^+$, whereas the non-*ansa* counterpart is a classical trihydride $[Cp^*_2Mo(H)_3]^+$. Further evidence in support of this view is provided by experiments to determine the magnitude of the J_{HD} coupling constant in isotopologues.

Evidence for Nonclassical Character of $\{[Me_2Si(C_5Me_4)_2]Mo(\eta^2\text{-}H_2)(H)\}^+$ Based on the Magnitude of J_{HD}. The magnitude of J_{HD} in polyhydride compounds has been shown to exhibit a roughly linear inverse correlation with H−H distance for short H−H distances,[3c,34,35] such that the value of J_{HD} provides a means to assess the nonclassical nature of a complex; viz., classical hydride complexes are typically characterized by values of $^2J_{HD}$ that are less than 5 Hz, whereas nonclassical hydride complexes with a direct H−H bond are typically characterized by values that are >15 Hz (for comparison, the $^1J_{HD}$ coupling constant in HD is 43 Hz). Verification that $\{[Me_2Si(C_5Me_4)_2]MoH_3\}^+$ exists as the nonclassical dihydrogen−

(32) At 500 MHz, the relaxation rate constant for two protons separated by a distance r Å is given by the expression $R_{HH} = (77.51/r^6)$ Å^6 s^{-1}, while components provided by interaction with ^{95}Mo and ^{97}Mo nuclei are given by the expressions $R_{HX} = (2.756/r^6)$ Å^6 s^{-1} for X = ^{95}Mo (15.72% abundance) and $R_{HX} = (2.872/r^6)$ Å^6 s^{-1} for X = ^{97}Mo (16.53% abundance). See ref 29.

(33) The calculated T_1(min) values for the dihydrogen complexes assume that the H_2 ligand is not rotating, which is in accord with the low-temperature NMR studies on the isotopologues $\{[Me_2Si(C_5Me_4)_2]MoH_2D\}^+$ and $\{[Me_2Si(C_5Me_4)_2]MoHD_2\}^+$ (see text). If the H_2 ligand were to be rapidly rotating, the T_1(min) component associated with the H−H relaxation is a factor of 4 longer than that in the absence of rotation. See: (a) Bautista, M. T.; Earl, K. A.; Maltby, P. A.; Morris, R. H.; Schweitzer, C. T.; Sella, A. *J. Am. Chem. Soc.* **1988**, *110*, 7031−7036. (b) Morris, R. H.; Wittebort, R. J. *Magn. Reson. Chem.* **1997**, *35*, 243−250. (c) Gusev, D. G.; Kuhlman, R. L.; Renkema, K. B.; Eisenstein, O.; Caulton, K. G. *Inorg. Chem.* **1996**, *35*, 6775−6783. (d) Bautista, M. T.; Capellani, E. P.; Drouin, S. D.; Morris, R. H.; Schweitzer, C. T.; Sella, A.; Zubkowski, J. P. *J. Am. Chem. Soc.* **1991**, *113*, 4876−4887 (ref 48).

(34) (a) Maltby, P. A.; Schlaf, M.; Steinbeck, M.; Lough, A. J.; Morris, R. H.; Klooster, W. T.; Koetzle, T. F.; Srivastava, R. C. *J. Am. Chem. Soc.* **1996**, *118*, 5396−5407. (b) Heinekey, D. M.; Luther, T. A. *Inorg. Chem.* **1996**, *35*, 4396−4399. (c) Earl, K. A.; Jia, G. C.; Maltby, P. A.; Morris, R. H. *J. Am. Chem. Soc.* **1991**, *113*, 3027−3039. (d) Klooster, W. T.; Koetzle, T. F.; Guochen, J.; Fong, T. P.; Morris, R. H.; Albinati, A. *J. Am. Chem. Soc.* **1994**, *116*, 7677−7681. (e) Hush, N. S. *J. Am. Chem. Soc.* **1997**, *119*, 1717−1719.

(35) Note that curvature in such plots is observed for longer H···H separations. See: Gründemann, S.; Limbach, H.-H.; Buntkowsky, G.; Sabo-Etienne, S.; Chaudret, B. *J. Phys. Chem. A* **1999**, *103*, 4752−4754.

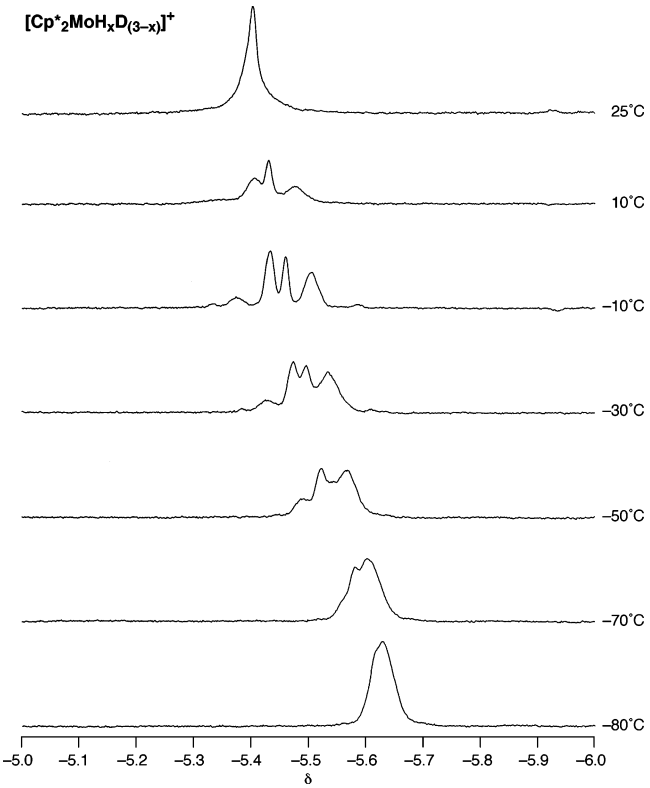

Figure 3. Temperature dependence of the hydride region of a mixture of $[Cp^*_2MoH_xD_{(3-x)}]^+$ isotopologues. Upon lowering the temperature from 25 °C, the spectrum decoalesces into a complex pattern, but recoalesces upon further cooling. The unusual temperature dependence is a manifestation of two effects, namely (i) the influence of temperature on the rate of central and lateral hydride ligand exchange and (ii) the influence of temperature on the chemical shifts of the central and lateral hydride ligands.

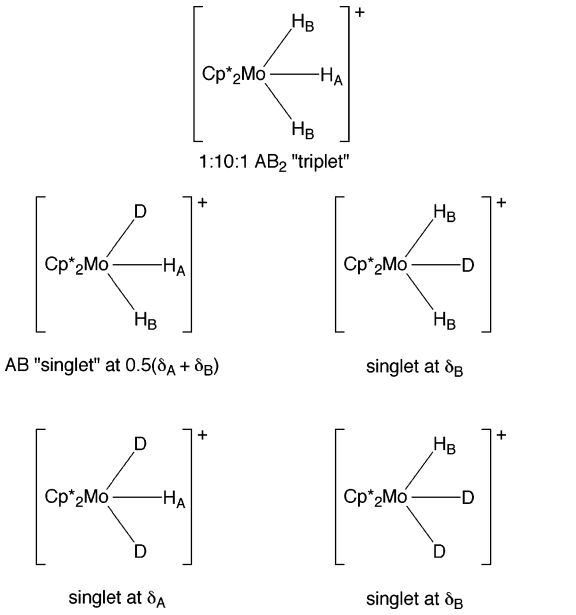

Figure 4. ^{1}H NMR hydride signals predicted for the various isotopologues and isotopomers of static $[Cp^*_2MoH_xD_{(3-x)}]^+$. (i) $[Cp^*_2MoH_3]^+$ is characterized by a 1:10:1 AB_2 triplet due to a large quantum mechanical exchange coupling; (ii) $[Cp^*_2MoH_2D]^+$ consists of two isotopomers in the statistical ratio of 2:1, each of which is characterized by a singlet. The isotopomer with deuterium in the central site is characterized by a singlet at the chemical shift corresponding to that of the lateral site, while the isotopomer with deuterium in the lateral site is characterized by a singlet at the average chemical shift of the central and lateral sites (i.e. a highly second-order AB pattern since $J_{AB} \gg \Delta_{AB}$ due to quantum mechanical exchange coupling); (iii) $[Cp^*_2MoHD_2]^+$ is composed of two isotopomers in the statistical ratio of 2:1, each of which is characterized by a singlet at the chemical shift of the lateral and central sites, respectively.

hydride isomer $\{[Me_2Si(C_5Me_4)_2]Mo(\eta^2\text{-}H_2)(H)\}^+$ was, therefore, sought by measurement of J_{HD} in the isotopologues $\{[Me_2Si(C_5Me_4)_2]MoH_2D\}^+$ and $\{[Me_2Si(C_5Me_4)_2]MoHD_2\}^+$.

(i) Variable-Temperature ^{1}H NMR Spectroscopic Properties of $[Cp^*_2MoH_3]^+$, $[Cp^*_2MoH_2D]^+$, and $[Cp^*_2MoHD_2]^+$. Prior to discussing isotopologues of $\{[Me_2Si(C_5Me_4)_2]MoH_3\}^+$, it is pertinent to consider those of the non-*ansa* system, $[Cp^*_2MoH_3]^+$. At room temperature, the hydride region of an isotopic mixture of $[Cp^*_2MoH_3]^+$, $[Cp^*_2MoH_2D]^+$, and $[Cp^*_2MoHD_2]^+$ is composed of a single resonance that is devoid of any resolvable J_{HD} coupling (Figure 3). The observation of a single resonance is consistent with a fluxional classical trihydride structure for each isotopologue with a small (unresolvable) $^2J_{HD}$ coupling constant for $[Cp^*_2MoH_2D]^+$ and $[Cp^*_2MoHD_2]^+$; it also indicates that the intrinsic isotope effect on chemical shift is small for this system.

Although the room-temperature hydride regions of the ^{1}H NMR spectra of $[Cp^*_2MoH_3]^+$, $[Cp^*_2MoH_2D]^+$, and $[Cp^*_2MoHD_2]^+$ are indistinguishable, interesting differences are, nevertheless, observed as the temperature is lowered. Thus, as illustrated in Figure 3, the single resonance corresponding to an isotopic mixture of $[Cp^*_2MoH_3]^+$, $[Cp^*_2MoH_2D]^+$, and $[Cp^*_2MoHD_2]^+$ at room temperature decoalesces into a complex six-line pattern at −10 °C; upon further cooling, however, the complex six-line pattern recoalesces into a single peak at −80 °C! This unusual temperature dependence is a manifestation of two effects, namely (i) the influence of temperature on the rate of central and lateral hydride ligand exchange and (ii) the influence of temperature on the chemical shifts of the central and lateral hydride ligands.

At room temperature, the NMR spectrum of the hydride region is a singlet for each isotopologue because chemical exchange between the central and lateral hydride sites is rapid. Upon lowering the temperature to −10 °C, chemical exchange becomes sufficiently slow that a static spectrum is observed for each of the isotopologues. Each isotopologue, however, exhibits its own distinct pattern (Figure 4), and thus as the temperature is lowered to −10 °C, the singlet for the mixture of $[Cp^*_2MoH_3]^+$, $[Cp^*_2MoH_2D]^+$, and $[Cp^*_2MoHD_2]^+$ at room temperature decoalesces into the complex pattern corresponding to a superposition of the individual spectra of the three isotopologues (Figure 5).

Upon further cooling the signals start to recoalesce because the chemical shifts of the central and lateral sites are temperature dependent (Figure 1). Thus, as the temperature is lowered, the chemical shifts of the central and lateral hydride sites approach a common value, with the result that all lines appear to merge into a single peak.[36] The influence of temperature on the fluxionality and chemical shifts of the central and lateral hydride sites, therefore, explains the unusual temperature dependence of the isotopologues of $[Cp^*_2MoH_3]^+$. It is important to note that a J_{HD} coupling is not resolvable at any temperature and thereby reinforces the notion that $[Cp^*_2Mo(H)_3]^+$ is a classical trihydride.

(36) The satellites of the 1:10:1 $[Cp^*_2MoH_3]^+$ are no longer observable because it represents only a minor component of the isotopic mixture and the recoalesced peak is broad.

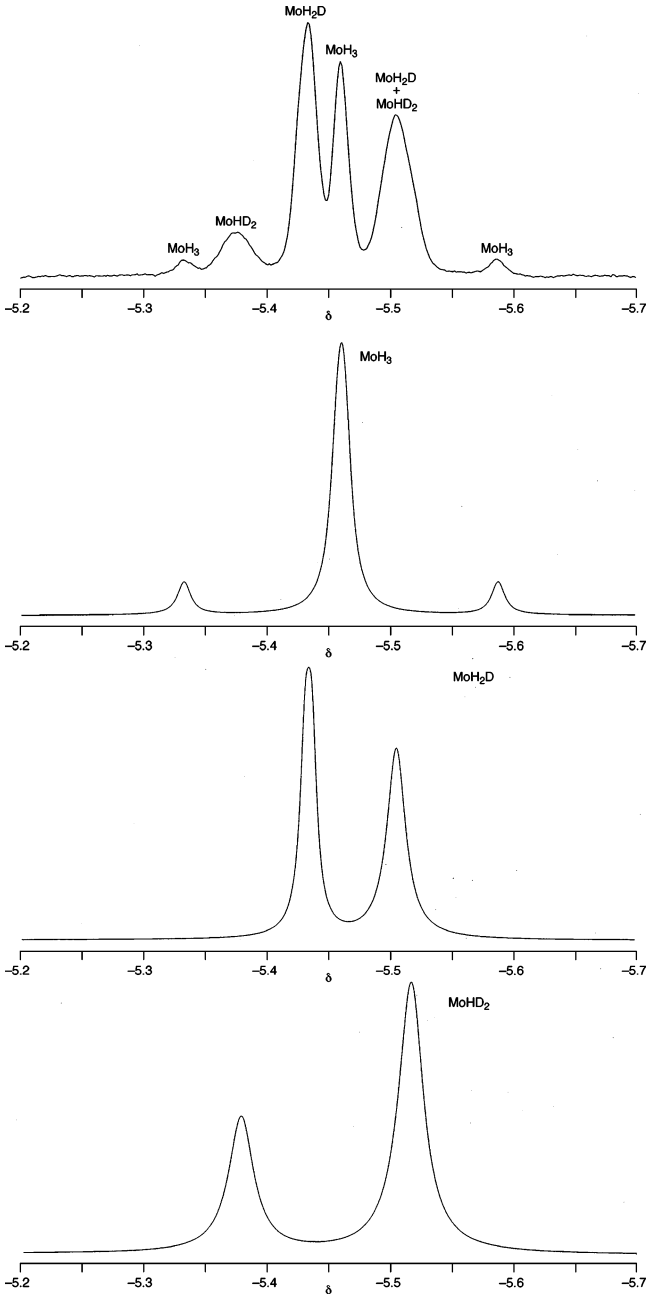

Figure 5. Simulated spectra of the hydride region of the ^{1}H NMR spectrum of $[Cp^*_2MoH_3]^+$, $[Cp^*_2MoH_2D]^+$, and $[Cp^*_2MoHD_2]^+$ isotopologues and a 1.00:0.67:0.67 mixture at −10 °C.

(ii) Variable-Temperature ^{1}H NMR Spectroscopic Properties of $\{[Me_2Si(C_5Me_4)_2]MoH_3\}^+$, $\{[Me_2Si(C_5Me_4)_2]MoH_2D\}^+$, and $\{[Me_2Si(C_5Me_4)_2]MoHD_2\}^+$. The hydride region of the ^{1}H NMR spectrum of a mixture of the isotopologues of the *ansa* complexes $\{[Me_2Si(C_5Me_4)_2]MoH_3\}^+$, $\{[Me_2Si(C_5Me_4)_2]MoH_2D\}^+$, and $\{[Me_2Si(C_5Me_4)_2]MoHD_2\}^+$ (Figure 6) provides a marked contrast to that of the non-*ansa* system. For example, whereas a single resonance is observed at room temperature for the non-*ansa* system, each isotopologue in the *ansa* system is characterized by a distinct signal: a singlet at −5.44 ppm corresponding to $\{[Mo]H_3\}^+$, a triplet at −5.49 ppm ($J_{HD(obs)} = 8.0$ Hz) corresponding to $\{[Mo]H_2D\}^+$, and a quintet at −5.58 ppm ($J_{HD(obs)} = 7.8$ Hz) corresponding to $\{[Mo]HD_2\}^+$ ([Mo] = $[Me_2Si(C_5Me_4)_2]Mo$). Since $\{[Me_2Si(C_5Me_4)_2]MoH_xD_{(3-x)}\}^+$ is fluxional, the values of $J_{HD(obs)}$ correspond to an appropriately weighted average of the J_{HD} coupling constants for each isotopologue. The magnitude of $J_{HD(obs)}$ is, nevertheless, consistent with its formulation as a nonclassical dihydrogen−hydride complex $\{[Me_2Si(C_5Me_4)_2]Mo(\eta^2\text{-}H_2)(H)\}^+$. For example, *if* (i) the fluxionality involved only intramolecular exchange within a dihydrogen−hydride species for which $^2J_{HD} \approx 0$, and (ii) there is no isotopic preference for deuterium to occupy a particular site, the observed values of $J_{HD(obs)}$ are statistically reduced from the value of $^1J_{HD}$ in the corresponding η^2-HD ligand to a value of 0.333 $^1J_{HD}$. On this basis, $^1J_{HD}$ would be predicted to be 24.0 Hz for $\{[Me_2Si(C_5Me_4)_2]MoH_2D\}^+$ and 23.4 Hz for $\{[Me_2Si(C_5Me_4)_2]MoHD_2\}^+$, values that are consistent with the presence of an η^2-HD ligand.[3c,34,3737]

Most interestingly, the variable-temperature behavior of the $\{[Me_2Si(C_5Me_4)_2]MoH_xD_{(3-x)}\}^+$ isotopologues is also quite distinct from that of the $[Cp^*_2MoH_xD_{(3-x)}]^+$ system. Thus, while the hydride region of the ^{1}H NMR spectrum of $\{[Me_2Si(C_5Me_4)_2]MoH_3\}^+$ remains as a single resonance over the temperature range 20 to −80 °C (500 MHz), the isotopologues $\{[Me_2Si(C_5Me_4)_2]MoH_2D\}^+$ and $\{[Me_2Si(C_5Me_4)_2]MoHD_2\}^+$ exhibit decoalescence (Figure 7). Comparison of the ^{1}H NMR spectra of samples with various isotopic enrichments enables assignment of the resonances attributed to each isotopomer in the low-temperature (−95 °C) 300 MHz NMR spectra, as illustrated in Figure 8. Thus, (i) the $\{[Mo]H_3\}^+$ isotopologue is characterized by a singlet at −5.78 ppm, (ii) the $\{[Mo]H_2D\}^+$ isotopologue is characterized by a broad singlet at −5.61 ppm and a 1:1:1 triplet ($J_{HD(obs)} = 13.4$ Hz) at −6.46 ppm, and (iii) the $\{[Mo]HD_2\}^+$ isotopologue is characterized by two broad resonances at −5.00 ppm ($J_{HD(obs)} \approx 13.2$ Hz) and −6.50 ppm.

The observation of *two* signals for each of the $\{[Mo]H_2D\}^+$ and $\{[Mo]HD_2\}^+$ isotopologues is inconsistent with a static dihydrogen−hydride structure which would be characterized by

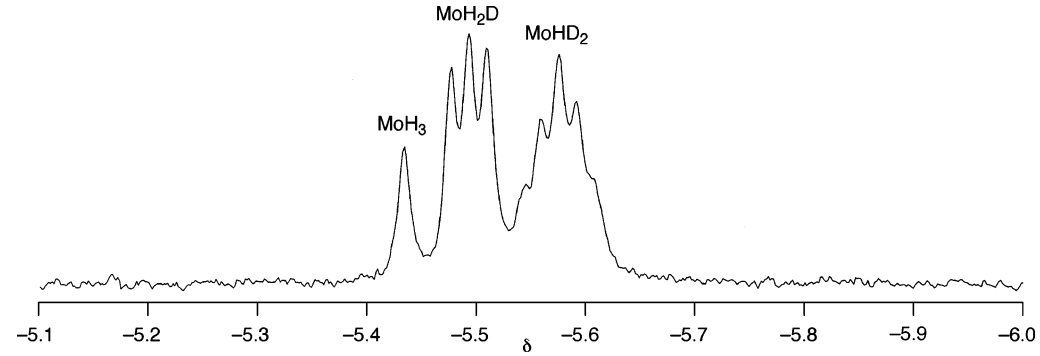

Figure 6. ^{1}H NMR spectrum (500 MHz) of the hydride region of a mixture of $\{[Me_2Si(C_5Me_4)_2]MoH_xD_{(3-x)}\}^+$ isotopologues at 25 °C.

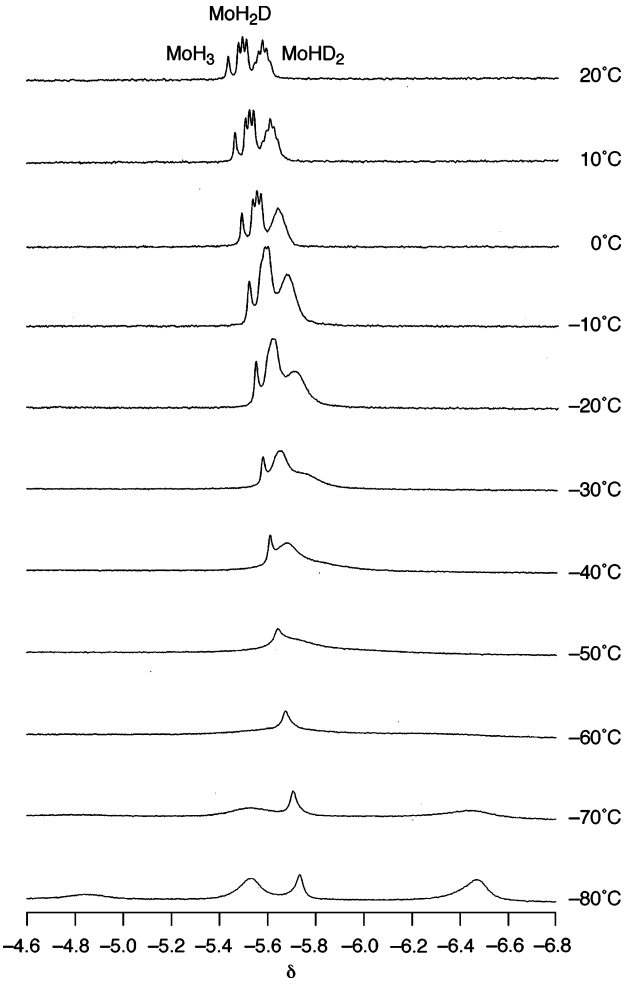

Figure 7. Variable-temperature ^{1}H NMR spectrum (500 MHz) of the hydride region of a mixture of $\{[Me_2Si(C_5Me_4)_2]MoH_xD_{(3-x)}\}^+$ isotopologues.

Scheme 2. Predicted Chemical Shifts for Isotopomers of $\{[Me_2Si(C_5Me_4)_2]MoH_2D\}^+$[a]

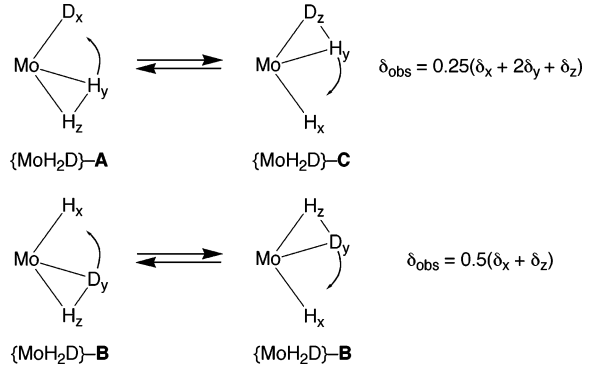

[a] Rapid "side-to-side" interconversion between $\{MoH_2D\}$–**A** and $\{MoH_2D\}$–**C** achieves site exchange between H_x and H_z such that the $\{MoH_2D\}$–**A**/$\{MoH_2D\}$–**C** isotopomeric mixture would be characterized by resonances at $0.5(\delta_x + \delta_z)$ and δ_y; however, the presence a large J_{yz} coupling constant causes the mixture to be characterized by a single resonance at $0.25(\delta_x + 2\delta_y + \delta_z)$. Rapid "side-to-side" motion within $\{MoH_2D\}$–**B** achieves site exchange between H_x and H_z such that the isotopomer is characterized by a single resonance at $0.5(\delta_x + \delta_z)$.

three signals, namely the hydride (H_x) and the *endo* (H_y) and *exo* (H_z) hydrogen atoms of the dihydrogen ligand. It is, therefore, evident that the fluxionality is not fully quenched at −95 °C; the spectra are, nevertheless, fully consistent with the notion that the rotation of the H_2 ligand (i.e. H_y/H_z site interconversion) has been frozen, while the "side-to-side" process involving H−H bond cleavage and H−H bond formation, resulting in H_x/H_z site interconversion, is still facile (Schemes 2 and 3).

Scheme 3. Predicted Chemical Shifts for Isotopomers of $\{[Me_2Si(C_5Me_4)_2]MoHD_2\}^+$[a]

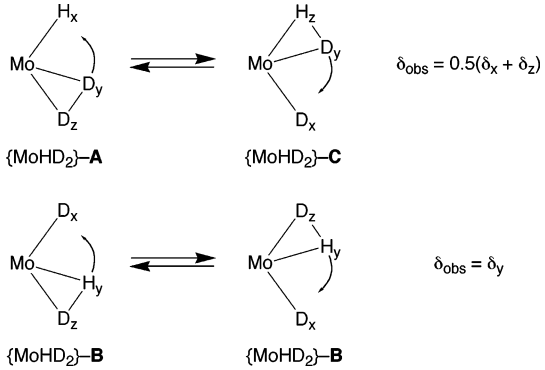

[a] Rapid "side-to-side" interconversion between $\{MoHD_2\}$–**A** and $\{MoHD_2\}$–**C** achieves site exchange between H_x and H_z such that the $\{MoHD_2\}$–**A**/$\{MoHD_2\}$–**C** isotopomeric mixture is characterized by a resonance at $0.5(\delta_x + \delta_z)$. Rapid "side-to-side" motion within $\{MoHD_2\}$–**B** results in no site exchange such that the isotopomer is characterized by a single resonance at δ_y.

Another important aspect of the low-temperature NMR spectra is that J_{HD} coupling is evident in some of the signals. Most notably, the signal at −6.46 ppm corresponding to $0.5(\delta_x + \delta_z)$ of the $\{[Mo]H_2D\}^+$ isotopologue is a 1:1:1 triplet with $J_{HD(obs)} = 13.4$ Hz. As a result of the "side-to-side" exchange process, $J_{HD(obs)}$ is not equal to $^1J_{HD}$ for the η^2-HD ligand; however, a value of $^1J_{HD} = 26.8$ Hz may be estimated if it is assumed that $^2J_{HD} \approx 0$, such that $J_{HD(obs)} = 0.5\ ^1J_{HD}$.

In contrast to the 1:1:1 triplet for $\{[Mo]H_2D\}^+$, the corresponding signal at −6.50 ppm for $0.5(\delta_x + \delta_z)$ of the $\{[Mo]HD_2\}^+$ isotopologue exhibits *no* observable coupling. If the signal at −6.50 ppm for $\{[Mo]HD_2\}^+$ were also to be a 1:1:1 triplet, it is evident that it should be resolvable to a similar degree to that for the $\{[Mo]H_2D\}^+$ isotopomer. Indeed, a quintet coupling is observable, although not well resolved, for the signal at −5.00 ppm corresponding to δ_y; a value of $J_{HD(obs)} = 13.2$ Hz, comparable to that observed for the 1:1:1 triplet for $\{[Mo]H_2D\}^+$ isotopologue (13.4 Hz), is determined using resolution enhancement. A rationalization for the absence of coupling in the signal at −6.50 ppm for $\{[Mo]HD_2\}^+$ is provided by the possibility that the two deuterium atoms of the $\{Mo(\eta^2\text{-}D_2)(H)\}^+$ isotopomer exhibit a large D−D quantum mechanical exchange coupling. Such a coupling would be manifested in the ^{1}H NMR spectrum by the proton coupling equally to *both* deuterium nuclei with $J_{HD(obs)} = 0.25J_{HD}$.[38] The reduced coupling constant thus provides an explanation for the fact that the signal at −6.50 ppm for the $\{[Mo]HD_2\}^+$ isotopologue appears as a singlet, whereas coupling is observed

(37) Alternatively, if the fluxionality involved only central/lateral hydride site exchange within a trihydride species with a common $^2J_{HD}$ coupling constant, the value of $J_{HD(obs)}$ would be equal to that of $^2J_{HD}$. Since classical hydride complexes are characterized by values of $^2J_{HD}$ that are less than 5 Hz, it is evident that the values of $J_{HD(obs)}$ are not consistent with a classical formulation.

(38) The situation is an example of "virtual coupling" in ABX systems, for which the X portion (i.e. H in the present case) *appears* to couple equally to A and B if J_{AB} is large even though $J_{AX} \neq J_{BX}$. See for example: Günther, H. *NMR Spectroscopy: Basic Principles, Concepts and Applications in Chemistry*, 2nd ed.; John Wiley & Sons: New York, 1994; p179.

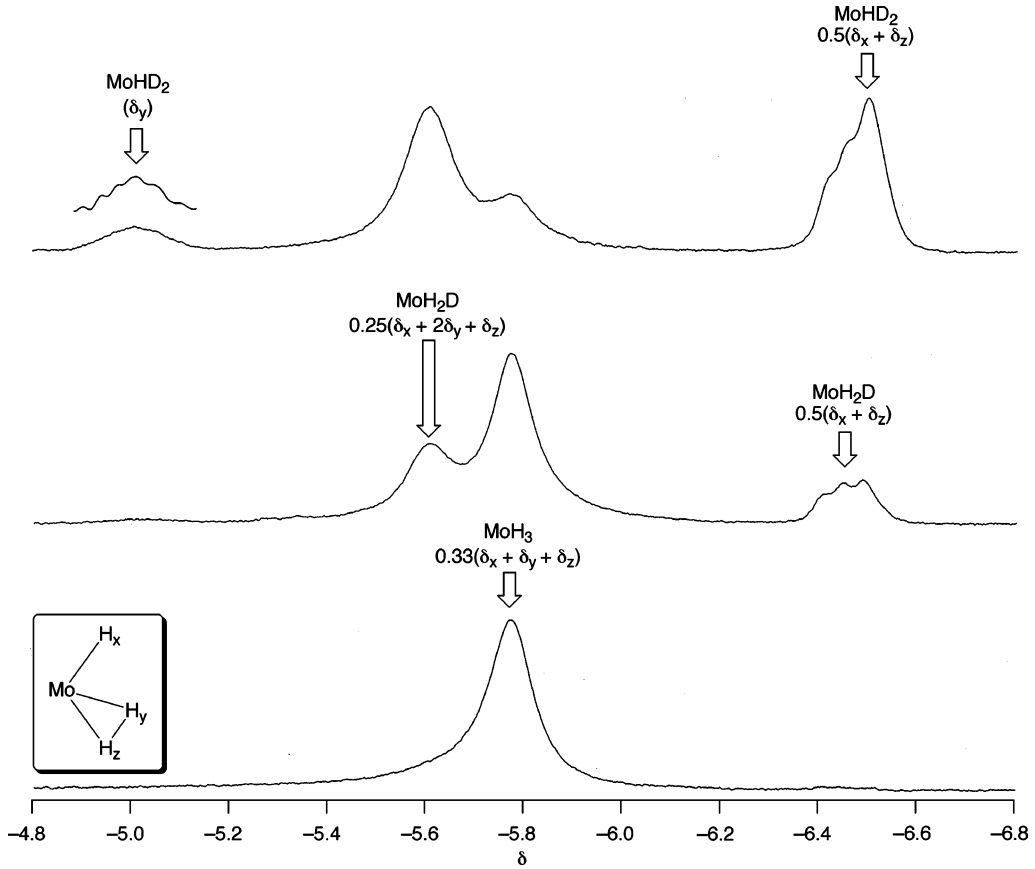

Figure 8. Comparison of the low-temperature (−95 °C) ^{1}H NMR (300 MHz) spectra of $\{[Me_2Si(C_5Me_4)_2]MoH_3\}^+$ (lower trace) with $\{[Me_2Si(C_5Me_4)_2]MoH_2D\}^+$ (middle trace) and a mixture of $\{[Me_2Si(C_5Me_4)_2]MoH_2D\}^+$ and $\{[Me_2Si(C_5Me_4)_2]MoHD_2\}^+$ (upper trace). The inset resonance corresponding to δ_y for $MoHD_2$ in the upper trace is the result of resolution enhancement.

in the signal at −5.00 ppm for $\{[Mo]HD_2\}^+$ and −6.46 ppm for $\{[Mo]H_2D\}^+$, for which $J_{HD(obs)} = 0.5J_{HD}$. Seminal studies by Heinekey and Zilm[12] and by Weitekamp[11] have firmly established the manifestation of quantum mechanical exchange coupling between protons in ^{1}H NMR spectroscopy, but few reports have described exchange coupling between deuterium nuclei.[13] A large D−D exchange coupling has, however, been suggested by Chaudret to explain the fact that the hydride region of the ^{2}H NMR spectrum of $[Cp_2Ta(\eta^2\text{-}D_2)CO]^+$ is a singlet, whereas that for $[Cp_2Ta(\eta^2\text{-}HD)CO]^+$ exhibits independent signals for two isotopomers.[39]

The values of $^1J_{HD}$ for the $\{[Mo]H_2D\}^+$ (26.8 Hz) and $\{[Mo]HD_2\}^+$ (26.4 Hz) isotopologues may be used to determine the H−H distance within $\{[Me_2Si(C_5Me_4)_2]Mo(\eta^2\text{-}H_2)(H)\}^+$ by application of the empirical correlation between d_{HH} and $^1J_{HD}$, i.e. $d_{HH} = 1.42 - 0.0167J_{HD}$.[34a] Thus, using the average value of 26.6 Hz for $^1J_{HD}$, the H−H distance for $\{[Me_2Si(C_5Me_4)_2]Mo(\eta^2\text{-}H_2)(H)\}^+$ is estimated to be 0.98 Å. The value of $^1J_{HD}$ thereby provides excellent experimental evidence for the dihydrogen−hydride formulation, and the derived H−H bond length is in good agreement with the geometry optimized value of 0.90 Å (vide infra).

Barrier to Rotation of the Coordinated H_2 Ligand in $\{[Me_2Si(C_5Me_4)_2]Mo(\eta^2\text{-}H_2)(H)\}^+$. The rotation of dihydrogen ligands is generally characterized by small activation barriers (<3 kcal mol^{-1});[3,40] for example, the barrier to rotation in $W(CO)_3(PCy_3)_2(\eta^2\text{-}H_2)$ is 1.9 kcal mol^{-1}, as determined by inelastic neutron scattering experiments.[41] An important aspect of the low-temperature ^{1}H NMR spectra of the $\{[Me_2Si(C_5Me_4)_2]MoH_2D\}^+$ and $\{[Me_2Si(C_5Me_4)_2]MoHD_2\}^+$ isotopologues is that they provide examples in which rotation of the HD ligand is frozen on the NMR time scale. In this regard, Chaudret recently provided the first evidence that such rotation may be blocked on the NMR time scale by demonstrating that the two different rotamers of $[(Cp^{TMS})_2Nb(\eta^2\text{-}HD)(PMe_2Ph)]^+$, differentiated according to whether deuterium occupied the central or lateral site, do not interconvert on the NMR time scale at −70 °C.[42] Shortly thereafter, the related niobocene $[(Cp^{TMS})_2Nb(\eta^2\text{-}HD)(CNR)]^+$ (R = Bu^t, Cy, Xyl)[43] and tantalocene complexes $[Cp_2Ta(\eta^2\text{-}HD)(CO)]^+$[39] were also shown to exhibit hindered rotation. More recently, Green, Green, and Heinekey have observed the hindered rotation of dihydrogen in isotopologues of $\{[Me_2C(C_5H_4)_2]Mo(\eta^2\text{-}H_2)(H)\}^+$,[27] analogous to that reported here for $\{[Me_2Si(C_5Me_4)_2]Mo(\eta^2\text{-}H_2)(H)\}^+$.

(39) (a) Sabo-Etienne, S.; Rodriguez, V.; Donnadieu, B.; Chaudret, B.; el Makarim, H. A.; Barthelat, J.-C.; Ulrich, S.; Limbach, H. H.; Möise, C. *New J. Chem.* **2001**, *25*, 55−62. (b) Sabo-Etienne, S.; Chaudret, B.; el Makarim, H. A.; Barthelat, J.-C.; Daudey, J.-P.; Ulrich, S.; Limbach, H. H.; Möise, C. *J. Am. Chem. Soc.* **1995**, *117*, 11602−11603.

(40) Eckert, J. *Trans. Am. Crystallogr. Assoc.* **1997**, *31*, 45−55.

(41) The value of 1.9 kcal mol^{-1} is lower than that originally reported (2.2 kcal mol^{-1}) due to the use of a modified H−H distance [0.89(1) Å] determined by solid-state ^{1}H NMR spectroscopy. See: (a) Kubas, G. J.; Nelson, J. E.; Bryan, J. C.; Eckert, J.; Wisniewski, L.; Zilm, K. *Inorg. Chem.* **1994**, *33*, 2954−2960. (b) Eckert, J.; Kubas, G. J.; Hall, J. H.; Hay, P. J.; Boyles, C. M. *J. Am. Chem. Soc.* **1990**, *112*, 2324−2332.

(42) Jalón, F. A.; Otero, A.; Manzano, B. R.; Villaseñor, E.; Chaudret, B. *J. Am. Chem. Soc.* **1995**, *117*, 10123−10124.

(43) Antiñolo, A.; Carrillo-Hermosilla, F.; Fajardo, M.; Garcia-Yuste, S.; Otero, A.; Camanyes, S.; Maseras, F.; Moreno, M.; Lledós, A.; Lluch, J. M. *J. Am. Chem. Soc.* **1997**, *119*, 6107−6114.

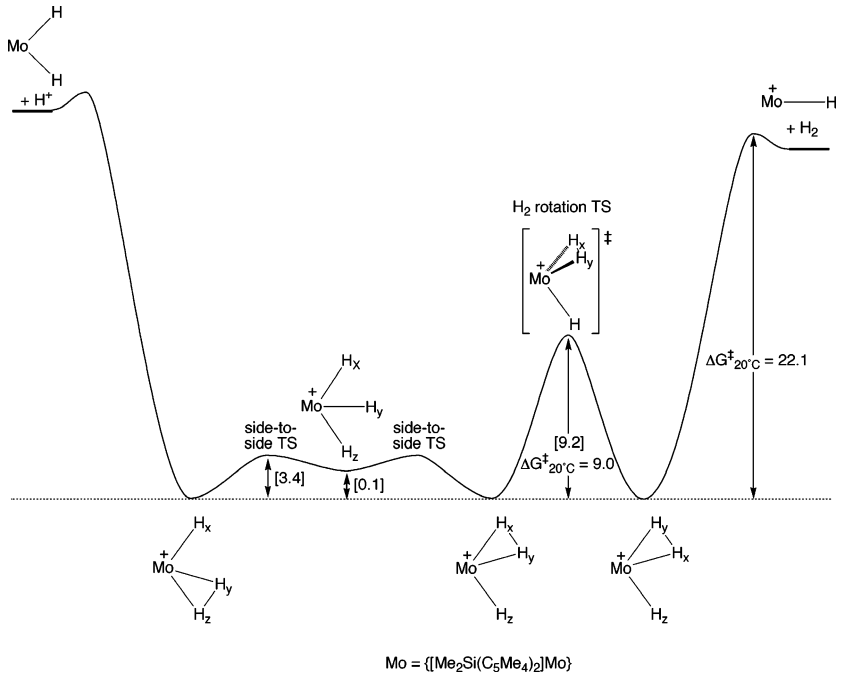

Figure 9. Semiquantitative energy surface (kcal mol^{-1}) pertaining to $\{[Me_2Si(C_5Me_4)_2]MoH_3\}^+$. Values in brackets correspond to calculated $\Delta H^{SCF(solv)}$.

Table 4. Comparison of Activation Barriers for Rotation of HD Ligand As Measured by ^{1}H NMR Spectroscopy

	T/°C	$\Delta G^{\ddagger}$/ kcal mol^{-1}	ref
$[(Cp^{TMS})_2Nb(\eta^2\text{-HD})(PMe_2Ph)]^+$	−40	11.2	42
$[(Cp^{TMS})_2Nb(\eta^2\text{-HD})(CNBu^t)]^+$	−80	8.9	43
$[(Cp^{TMS})_2Nb(\eta^2\text{-HD})(CNCy)]^+$	−75	9.1	43
$[(Cp^{TMS})_2Nb(\eta^2\text{-HD})(CNXyl)]^+$	−90	8.4	43
$[Cp_2Ta(\eta^2\text{-H}_2)(CO)]^+$	−65	9.6	39a
$\{[Me_2C(C_5H_4)_2]Mo(\eta^2\text{-HD})(D)\}^+$	−123	7.4	19
$\{[Me_2Si(C_5Me_4)_2]Mo(\eta^2\text{-HD})(H)\}^+$	−50	9.3	this work

The barrier to rotation of the HD ligand in $\{[Me_2Si(C_5Me_4)_2]Mo(\eta^2\text{-HD})(H)\}^+$ has been determined by analysis of the line shapes of the *endo*-D and *exo*-D rotamers over the range −50 to −85 °C and is characterized by the activation parameters $\Delta H^{\ddagger} = 10.2(3)$ kcal mol^{-1} and $\Delta S^{\ddagger} = 4(2)$ eu. At 20 °C, $\Delta G^{\ddagger} = 9.0$ kcal mol^{-1}, as illustrated by the semiquantitative energy surface of Figure 9, comparable to the values that have been reported for other metallocene dihydrogen complexes that exhibit hindered rotation on the NMR time scale (Table 4). Furthermore, it is noteworthy that the dihydrogen complexes discovered so far to exhibit hindered rotation of a dihydrogen ligand on the NMR time scale with barriers >7 kcal mol^{-1} are all d^2 metallocene derivatives. The increased barrier to rotation of the H_2 ligand in metallocene complexes is presumably associated with the pronounced electronic and steric preferences of the metallocene fragment. For example, the three frontier orbitals of the metallocene moiety lie in the equatorial plane[44] and thus a dihydrogen ligand that is perpendicular to this plane is incapable of participating in a π-back-bonding interaction with these orbitals. Likewise, steric interactions between the dihydrogen ligand and the cyclopentadienyl ring subsituents disfavor a perpendicular orientation. By comparison, the electronic barrier to rotation of H_2 in more symmetric "octahedral" complexes such as $W(CO)_3(PCy_3)_2(\eta^2\text{-H}_2)$, with a d^6 configuration, is smaller than that for metallocene derivatives because of the availability of filled d orbitals that stabilize the transition state via back-bonding.

Another feature of the dihydrogen complexes listed in Table 4 which deserves comment is that the *appearance* of a nonrotating dihydrogen ligand is observed only for HD ligands and not for H_2 ligands. Thus, while the chemically distinct environment of the two ends of the dihydrogen ligand in these complexes may be detected by observing two rotamers of the HD ligand, the corresponding H_2 ligand appears as a singlet. Two possibilities have been considered to explain the significantly different ^{1}H NMR spectroscopic features of η^2-H_2 and η^2-HD isotopologues, namely (i) a large kinetic isotope effect and (ii) a large quantum mechanical exchange coupling constant for the η^2-H_2 species that is quenched for the η^2-HD counterpart.[39,42,43] Of these possibilities, the latter is considered to be the mechanism responsible for the observation of a single peak for the η^2-H_2 ligand of the aforementioned niobocene and tantalocene complexes on the basis of ^{2}H NMR spectroscopic studies on an η^2-D_2 counterpart.[39] Specifically, the η^2-D_2 ligand was also observed as a single resonance, analogous to that of the η^2-H_2 ligand, indicating that the η^2-H_2, η^2-HD, and η^2-D_2 ligands do not exhibit a monotonic trend with respect to their spectroscopic properties, thereby strongly suggesting that the differences cannot be rationalized in terms of a kinetic isotope effect. The observation that the η^2-H_2 and η^2-D_2 ligands are each characterized by a single resonance was thus proposed to be a manifestation of large J_{HH} and J_{DD} exchange coupling constants within the AB spin system of a static dihydrogen ligand which causes the spectrum to appear as a singlet.[21] In contrast, exchange coupling is quenched for the η^2-HD ligand because the exchange is a nondegenerate process[11−13] and so both rotamers of the static η^2-HD ligand are characterized by separate 1:1:1 triplet signals. Although this explanation for the

(44) (a) Green, J. C. *Chem. Soc. Rev.* **1998**, *27*, 263−271. (b) Lauher, J. W.; Hoffmann, R. *J. Am. Chem. Soc.* **1976**, *98*, 1729−1742. (c) Green, J. C.; Green, M. L. H.; Prout, C. K. *J. Chem. Soc., Chem. Commun.* **1972**, 421−422.

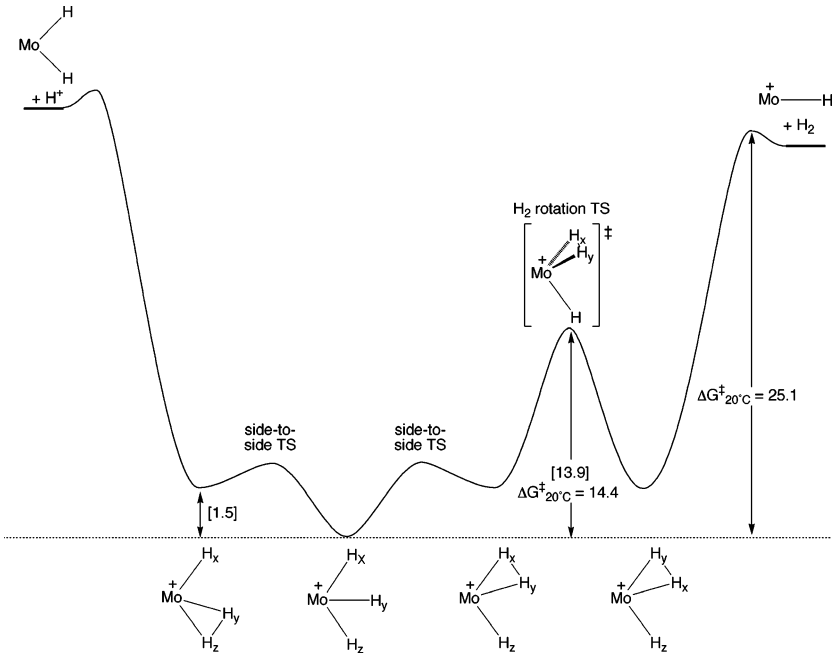

Figure 10. Semiquantitative energy surface (kcal mol^{-1}) pertaining to $[Cp^*_2MoH_3]^+$. Values in parentheses correspond to calculated $\Delta H^{SCF(solv)}$.

observation of a single resonance for a static H_2 ligand was originally proposed for $[MH_2]$ derivatives, a similar argument also rationalizes a singlet for $[MH_3]$ derivatives with an ABC spin system for the $[M(\eta^2\text{-}H_2)(H)]$ moiety in which there is a large J_{AB} coupling constant and facile A/C site exchange due to "side-to-side" motion of the central hydrogen.[22]

Finally, it is pertinent to compare the barrier to rotation of the HD ligand in $\{[Me_2Si(C_5Me_4)_2]Mo(\eta^2\text{-HD})(H)\}^+$ with the barrier to central/lateral site exchange of the hydride ligands in $[Cp^*_2MoH_3]^+$.[24] The data summarized in Table 4 demonstrate that the barrier to site exchange for $[Cp^*_2MoH_3]^+$ ($\Delta G^{\ddagger}_{(25°C)} =$ 14.3 kcal mol^{-1}) is substantially greater than that for the HD ligand in $\{[Me_2Si(C_5Me_4)_2]Mo(\eta^2\text{-HD})(H)\}^+$ ($\Delta G^{\ddagger}_{(25°C)} = 9.0$ kcal mol^{-1}), as illustrated in Figures 9 and 10. This difference in activation barriers corresponds to the significant factor of ~8000 in rate constant! However, it must be recognized that the comparison between $\{[Me_2Si(C_5Me_4)_2]Mo(\eta^2\text{-HD})(H)\}^+$ and $[Cp^*_2MoH_3]^+$ is not ideal because of a potential kinetic isotope effect. To determine the magnitude of the kinetic isotope effect on central/lateral site exchange, we have measured the barrier for site exchange within $[Cp^*_2MoHD_2]^+$. At each temperature, the rates of central/lateral site exchange for $[Cp^*_2MoHD_2]^+$ and $[Cp^*_2MoH_3]^+$ are of a comparable magnitude; for example, at 10 °C, $k_H/k_D = 0.9 \pm 0.2$, corresponding to a difference of only 0.05 kcal mol^{-1}.[45] The similarity of the barriers for site exchange within $[Cp^*_2MoH_3]^+$ and $[Cp^*_2MoHD_2]^+$ provides supporting evidence that the marked isotope effect on the NMR spectroscopic features associated with rotation of the dihydrogen ligand in $\{[Me_2Si(C_5Me_4)_2]Mo(\eta^2\text{-}H_2)(H)\}^+$ is *not* a manifestation of a simple kinetic isotope effect.

There are two factors that are responsible for the greater fluxionality of $\{[Me_2Si(C_5Me_4)_2]MoH_3\}^+$ compared to that of $[Cp^*_2MoH_3]^+$. Firstly, the steric demands in the front of the metallocene wedge are less for $\{[Me_2Si(C_5Me_4)_2]MoH_3\}^+$ because the $[Me_2Si]$ bridge causes the cyclopentadienyl rings to tilt more and thereby increases the distance between the ring methyl groups and the substituents in the equatorial plane; the reduced steric demands will facilitate hydride exchange because the process necessarily requires the "hydride" ligands to be displaced from the equatorial plane towards the ring methyl groups.[46] Secondly, since the exchange process is likely to involve close contact of the hydride ligands, another factor that would assist central and lateral "hydride" site exchange is the accessibility of a dihydrogen−hydride species. In this regard, a $[Me_2Si]$ bridge would be expected to facilitate the process by increasing the relative stability of the dihydrogen−hydride versus trihydride tautomer because the $[Me_2Si(C_5Me_4)_2]$ ligand is overall less electron-donating than two Cp* ligands,[17,26] and the equilibrium between classical and nonclassical hydrides is strongly influenced by such a factor.

Deuterium Site Preferences for $\{[Me_2Si(C_5Me_4)_2]MoH_2D\}^+$ and $\{[Me_2Si(C_5Me_4)_2]MoHD_2\}^+$. Another important aspect of the $\{[Me_2Si(C_5Me_4)_2]MoH_2D\}^+$ and $\{[Me_2Si(C_5Me_4)_2]MoHD_2\}^+$ isotopologues pertains to the relative preferences of deuterium and hydrogen to occupy hydride versus dihydrogen sites. In this regard, there are conflicting reports in the literature concerned with the site preference of deuterium, an observation that is not perhaps surprising given that equilibrium isotope effects involving small molecules such as H_2 are not always straightforwardly explained in terms of zero-point energy arguments.[47] For instance, experimental studies on $CpNb(CO)_3(\eta^2\text{-}H_2)$/$CpNb(CO)_3H_2$[48] and $[Re(PR_3)_3(CO)(\eta^2\text{-}H_2)H_2]^+$/$[Re(PR_3)_3(CO)H_4]^+$ ($PR_3 = PMe_2Ph$,[49] PMe_3[50]) indicate that deuterium favors the dihydrogen site, while studies on $[TpIr(PMe_3)(\eta^2\text{-}H_2)H]^+$ [7e,f] and

(45) In this regard, only a modest kinetic isotope effect of $k_H/k_D = 1.3$ has been reported for site exchange of $[\eta^4\text{-}P(CH_2CH_2PPh_2)_4]RhH_2$ and $[\eta^4\text{-}P(CH_2CH_2PPh_2)_4]Rh(H)(D)$. See: Heinekey, D. M.; van Roon, M. *J. Am. Chem. Soc.* **1996**, *118*, 12134−12140.

(46) Furthermore, we have previously noted that the barriers to rotation about the Zr−phenyl bond in a series of *ansa* complexes, namely $[Me_2Si(C_5Me_4)_2]Zr(Ph)X$ (X = H, Cl, Ph), are much lower than those for the corresponding $Cp^*_2Zr(Ph)X$ derivatives as a result of a reduced steric demands for the *ansa* system. See: Lee, H.; Bridgewater, B. M.; Parkin, G. *J. Chem. Soc., Dalton Trans.* **2000**, 4490−4493.

$[Cp_2W(\eta^2\text{-}H_2)H]^+$ [16] indicate that deuterium favors the hydride site; calculations on the tungsten complexes $W(CO)_3(L)_2(\eta^2\text{-}H_2)/W(CO)_3(L)_2H_2$ (L = CO[47g] and PH_3[51]), however, indicate that deuterium favors the dihydrogen site.

In principle, information pertaining to the site preference of deuterium could be obtained by analyzing the temperature dependence of the chemical shifts and J_{HD} coupling constants of the various isotopologues.[52] However, such an analysis is complicated by the fact that the observed changes may be due to several factors, or a composite thereof. Thus, the spectroscopic changes may be interpreted in terms of either (i) a temperature-dependent site preference for deuterium within the dihydrogen−hydride complex, (ii) a temperature-dependent equilibrium between the dihydrogen−hydride complex and the trihydride isomer, or (iii) a temperature-dependent variation in the length of the H−H bond.[53] For example, while the low-temperature ^{1}H NMR spectrum of the isotopic mixture of $\{[Me_2Si(C_5Me_4)_2]MoH_2D\}^+$ and $\{[Me_2Si(C_5Me_4)_2]MoHD_2\}^+$ provides convincing evidence for a dihydrogen−hydride formulation at −95 °C, it is not possible to know whether the ^{1}H NMR spectrum at room temperature corresponds to a single fluxional dihydrogen−hydride complex or a rapidly interconverting mixture of dihydrogen−hydride and trihydride species.

For simplicity, however, consider the situation in which $\{[Me_2Si(C_5Me_4)_2]Mo(\eta^2\text{-}H_2)(H)\}^+$ is the only species present at all temperatures. The ^{1}H NMR spectroscopic chemical shifts of the $\{[Me_2Si(C_5Me_4)_2]MoH_3\}^+$, $\{[Me_2Si(C_5Me_4)_2]MoH_2D\}^+$, and $\{[Me_2Si(C_5Me_4)_2]MoHD_2\}^+$ isotopologues shift to higher field [$\delta(H_3) = -5.44$, $\delta(H_2D) = -5.49$, $\delta(HD_2) = -5.58$] and the magnitudes of these shifts (0.05 and 0.09 ppm) are sufficiently great that they cannot be considered intrinsic isotope effects (recall that the related $[Cp^*_2MoH_xD_{3-x}]^+$ system exhibits no significant isotopic perturbation of chemical shift at room temperature). Assuming that the only species present is the dihydrogen−hydride complex, the observed difference in chemical shifts is consistent with two possible isotope effects, namely (i) deuterium favoring the dihydrogen site if the chemical shift of the hydride site is at higher field than that of the dihydrogen site, or (ii) deuterium favoring the hydride site if the chemical shift of the dihydrogen site is at higher field than that of the hydride site. Thus, while the observation of an isotopic perturbation of chemical shift provides a clear indication that deuterium exhibits a site preference, the direction of the isotopic perturbation in an exchange-averaged spectrum does not, per se, provide an indication as to whether deuterium favors the hydride or dihydrogen site; however, *if* the chemical shifts of the hydride and two dihydrogen sites were to be known, the direction of the isotopic perturbation of chemical shift would provide direct evidence for the site preference of deuterium. Unfortunately, the three required chemical shifts for $\{[Me_2Si(C_5Me_4)_2]Mo(\eta^2\text{-}H_2)(H)\}^+$ are not known; as described above, only the chemical shifts of the *endo* hydrogen of the η^2-H_2 ligand and the *average* of the hydride and *exo* hydrogen of the η^2-H_2 ligand are known.

In contrast to the direction of the isotopic perturbation of chemical shift, the isotopic perturbation of the $J_{HD(obs)}$ coupling constants in the exchange-averaged spectra of $\{[Me_2Si(C_5Me_4)_2]MoH_2D\}^+$ and $\{[Me_2Si(C_5Me_4)_2]MoHD_2\}^+$ does provide a direct means of establishing the site preference for deuterium. Specifically, a value of $J_{HD(obs)}[H_2D] > J_{HD(obs)}[HD_2]$ indicates that deuterium exhibits a greater than statistical preference to occupy the dihydrogen site, whereas a value of $J_{HD(obs)}[H_2D] < J_{HD(obs)}[HD_2]$ indicates that deuterium favors the hydride site.[54] Thus, the observation that $J_{HD(obs)}$ at 25 °C for $\{[Me_2Si(C_5Me_4)_2]MoH_2D\}^+$ (8.0 Hz) is slightly greater than that for the $\{[Me_2Si(C_5Me_4)_2]MoHD_2\}^+$ isotopologue (7.8 Hz) provides qualitative evidence that deuterium marginally favors the dihydrogen site within the dihydrogen−hydride complex; however, given the experimental uncertainty in these coupling constants (ca. ±0.5 Hz), it is evident that the data are incapable of providing a definitive statement concerning the site preference of deuterium.

In view of the experimental difficulty of measuring the site preference of deuterium in this system, we have calculated the site preference by using computational methods. Specifically, the equilibrium constants pertaining to the redistribution of isotopic labels within dihydrogen−hydride isotopologues $\{[Me_2Si(C_5Me_4)_2]MoH_2D\}^+$ and $\{[Me_2Si(C_5Me_4)_2]MoHD_2\}^+$ may be determined in a manner analogous to that used to determine equilibrium isotope effects in other systems.[47] Thus, the equilibrium constant may be expressed as $K = SYM{\cdot}MMI{\cdot}EXC{\cdot}ZPE$, where SYM is the symmetry factor, MMI is the mass−moment of inertia term, EXC is the excitation term, and ZPE is the zero-point energy term.[22,47] The SYM term is determined by the symmetry number ratio of the species involved; the MMI term is determined by their structures (i.e. their masses and moments of inertia); and the EXC and ZPE terms are determined by their vibrational frequencies. Frequency calculations are highly computationally intensive, however, and so it was necessary to perform such studies on a computationally simpler system in which the methyl groups of the $[Me_2Si(C_5Me_4)_2]$ ligand are replaced by hydrogen atoms, i.e. $\{[H_2Si(C_5H_4)_2]MoH_2D\}^+$ and $\{[H_2Si(C_5H_4)_2]MoHD_2\}^+$.

As noted above, there are two isotopomers of $\{[Me_2Si(C_5Me_4)_2]Mo(\eta^2\text{-}HD)(H)\}^+$ which differ according to whether the deuterium occupies the *endo* or *exo* site. Therefore, it was necessary to perform calculations on both *exo*-$\{[H_2Si(C_5H_4)_2]Mo(\eta^2\text{-}DH)(H)\}^+$ and *endo*-$\{[H_2Si(C_5H_4)_2]Mo(\eta^2\text{-}HD)(H)\}^+$. The calculations indicate that the two isotopomers have comparable energies, but that the isotopomer with deuterium in the *exo* site of the HD ligand is favored on enthalpic grounds.[22]

The temperature dependence of the equilibrium constants pertaining to the preference of deuterium to reside in the

(47) (a) Abu-Hasanayn, F.; Krogh-Jespersen, K.; Goldman, A. S. *J. Am. Chem. Soc.* **1993**, *115*, 8019−8023. (b) Bender, B. R.; Kubas, G. J.; Jones, L. H.; Swanson, B. I.; Eckert, J.; Capps, K. B.; Hoff, C. D. *J. Am. Chem. Soc.* **1997**, *119*, 9179−9190. (c) Slaughter, L. M.; Wolczanski, P. T.; Klinckman, T. R.; Cundari, T. R. *J. Am. Chem. Soc.* **2000**, *122*, 7953−7975. (d) Bender, B. R. *J. Am. Chem. Soc.* **1995**, *117*, 11239−11246. (e) Janak, K. E.; Parkin, G. *J. Am. Chem. Soc.* **2003**, *125*, 6889−6891. (f) Janak, K. E.; Parkin, G. *J. Am. Chem. Soc.* **2003**, *125*, 13219−13224. (g) Janak, K. E.; Parkin, G. *Organometallics* **2003**, *22*, 4378−4380. (h) Bullock, R. M.; Bender, B. R. Isotope Methods in Homogeneous Catalysis. In *Encyclopedia of Catalysis*; Horváth, I. T., Ed.; Wiley-Interscience: New York, 2003.
(48) Haward, M. T.; George, M. W.; Hamley, P.; Poliakoff, M. *J. Chem. Soc., Chem. Commun.* **1991**, 1101−1103.
(49) Luo, X.-L.; Crabtree, R. H. *J. Am. Chem. Soc.* **1990**, *112*, 6912−6918.
(50) Gusev, D. G.; Nietlispach, D.; Eremenko, I. L.; Berke, H. *Inorg. Chem.* **1993**, *32*, 3628−3636.
(51) Torres, L.; Moreno, M.; Lluch, J. M. *J. Phys. Chem. A* **2001**, *105*, 4676−4681.
(52) See, for example, refs 7e,f.
(53) Although the variation of H−H bond length with temperature has not been extensively documented, examples have been proposed in which it both increases[a] and decreases[b,c] with temperature. See: (a) Reference 34c. (b) Reference 34a. (c) Gelabert, R.; Moreno, M.; Lluch, J. M.; Lledos, A. *J. Am. Chem. Soc.* **1998**, *120*, 8168−8176.

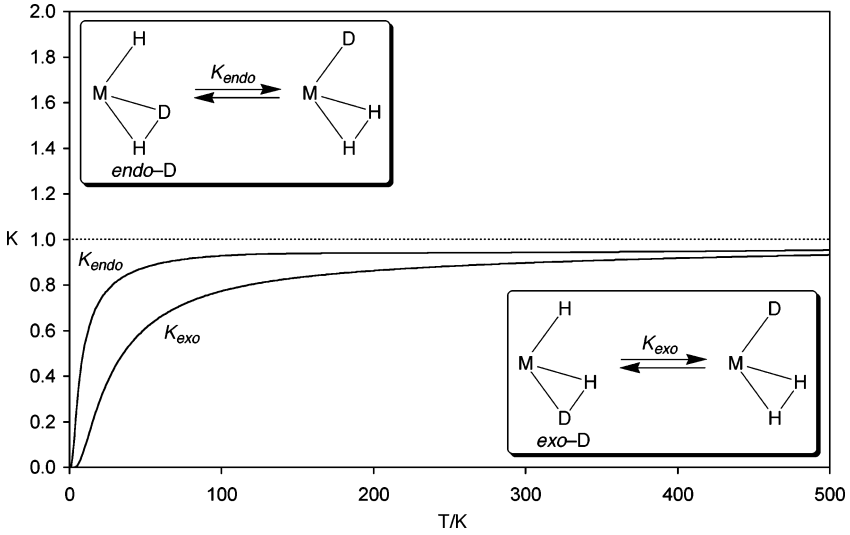

Figure 11. Calculated temperature dependence of the equilibrium constants for deuterium to occupy the hydride sites of d^1-{[$Me_2Si(C_5Me_4)_2$]Mo(η^2-H_2)(H)}$^+$.

dihydrogen versus hydride sites for both *exo-D*-{[$H_2Si(C_5H_4)_2$]Mo(η^2-DH)(H)}$^+$ and *endo-D*-{[$H_2Si(C_5H_4)_2$]Mo(η^2-HD)(H)}$^+$ is illustrated in Figure 11. In both cases, the equilibrium constants are such that deuterium prefers to reside in the dihydrogen site, supporting the proposal based on the observation that the room-temperature value of $J_{HD(obs)}$[H_2D] is greater than that of $J_{HD(obs)}$[HD_2]. Analysis of the individual SYM, MMI, EXC, and ZPE components indicates that the equilibrium constant is determined primarily by the ZPE term, which corresponds closely to the enthalpy component, [exp($-\Delta H/RT$)].[47f] The combined [SYM·MMI·EXC] term corresponds closely to the entropy component of the equilibrium constant, exp($\Delta\Delta S/R$), and is approximately unity at all temperatures. Calculations on the isotopomers of {[$H_2Si(C_5H_4)_2$]$MoHD_2$}$^+$ yield similar conclusions with respect to deuterium favoring the dihydrogen site for enthalpic reasons.[22]

Comparison of the Stability of {[$Me_2Si(C_5Me_4)_2$]Mo(η^2-H_2)(H)}$^+$ and [Cp*$_2$$MoH_3$]$^+$: Influence of a [$Me_2Si$] *Ansa* Bridge on Reductive Elimination of H_2. In addition to altering the classical/nonclassical nature of [Cp*$_2$$MoH_3$]$^+$ and {[$Me_2Si(C_5Me_4)_2$]Mo(η^2-H_2)(H)}$^+$, the [Me_2Si] *ansa* bridge also influences the stability of the complex with respect to elimination of H_2. Specifically, {[$Me_2Si(C_5Me_4)_2$]Mo(η^2-H_2)(H)}$^+$ eliminates H_2 rapidly at 20 °C with a first-order rate constant of 2.09(14) $\times$ 10^{-4} s^{-1} ($\Delta G^{\ddagger}$ = 22.1 kcal mol^{-1}),[55] whereas [Cp*$_2$$MoH_3$]$^+$ is much more thermally stable, with k = 6.48(14) $\times$ 10^{-7} s^{-1} ($\Delta G^{\ddagger}$ = 25.5 kcal mol^{-1}).[56] It is, therefore, evident that the [Me_2Si] *ansa* bridge promotes elimination of H_2 in this system by a factor of ~300 in rate constant. This observation bears a close analogy to our previous report that the [Me_2Si] bridge facilitates reductive elimination of H_2 from the related isoelectronic neutral d^0 tantalum system; viz., reductive elimination of H_2 from [$Me_2Si(C_5Me_4)_2$]TaH_3 is a factor of ~4000 faster than that from Cp*$_2$$TaH_3$.[57] The ability of a [$Me_2Si$] *ansa* bridge to facilitate elimination from {[$Me_2Si(C_5Me_4)_2$]Mo(η^2-H_2)(H)}$^+$ and [$Me_2Si(C_5Me_4)_2$]TaH_3 compared to their non-*ansa* counterparts is noteworthy in view of the fact that *ansa* bridges actually inhibit reductive elimination of methane in related systems, namely [$Me_2Si(C_5Me_4)_2$]W(Me)H[25c] and [$Me_2C(C_5H_4)_2$]W(Me)H.[15a,25a] An important distinction between these systems is concerned with the fact that reductive elimination from (Cp^R)$_2$W(Me)H derivatives generates a triplet tungstenocene intermediate that is more stable with a parallel ring structure.[58] An *ansa* bridge prevents access to a parallel ring geometry and thus hinders reductive elimination for (Cp^R)$_2$W(Me)H. In contrast, the initial product of reductive elimination of H_2 from trihydrides [(Cp^R)$_2$$MoH_3$]$^+$ is a monohydride [(Cp^R)$_2$MoH]$^+$ that is not expected to have a parallel ring structure and is thus not subject to the same factors. A simple rationalization for the ability of a [Me_2Si] bridge to promote reductive elimination in {[$Me_2Si(C_5Me_4)_2$]Mo(η^2-H_2)(H)}$^+$ is provided by the fact that the geometrical constraints associated with the bridge cause the *ansa* ligand to be overall less electron-donating than two cyclopentadienyl ligands.[17] As such, the *ansa* metallocene is less electron-rich and the higher oxidation state is not stabilized as effectively, with the result that reductive elimination is promoted.[59]

Comparison of the Acidity of [Cp*$_2$$Mo(H)_3$]$^+$ and {[$Me_2Si(C_5Me_4)_2$]Mo(η^2-H_2)(H)}$^+$: Influence of a [Me_2Si] *Ansa* Bridge on the Basicity of Molybdenocene Compounds. Another aspect of the influence of the [Me_2Si] bridge is

(54) For example, consider an extreme situation in which the preference for deuterium to occupy the dihydrogen site is 100%: {MoH_2D}$^+$ would exist as {Mo(η^2-HD)(H)}$^+$ with $J_{HD(obs)}$ = 0.5 $^1J_{HD}$ and {$MoHD_2$}$^+$ would exist as {Mo(η^2-D_2)(H)}$^+$ with $J_{HD(obs)}$ = 0. Conversely, if the preference for deuterium to occupy the hydride site is 100%: {MoH_2D}$^+$ would exist as {Mo(η^2-H_2)(D)}$^+$ with $J_{HD(obs)}$ = 0 and {$MoHD_2$}$^+$ would exist as {Mo(η^2-HD)(D)}$^+$ with $J_{HD(obs)}$ = 0.5 $^1J_{HD}$. A general relationship between $J_{HD(obs)}$[H_2D] and $J_{HD(obs)}$[HD_2] coupling constants may be expressed as {$J_{HD(obs)}$[H_2D]}/{$J_{HD(obs)}$[HD_2]} = [$2K + K^2$]/[1 + 2K], where K is a statistically uncorrected equilibrium constant between {Mo(η^2-HX)(D)}$^+$ and {Mo(η^2-DX)(H)}$^+$ (i.e. a value of K = 1 corresponds to no isotopic preference). From this expression, it is evident that a value of K > 1 (i.e. that deuterium favors the dihydrogen site) implies that $J_{HD(obs)}$[H_2D] > $J_{HD(obs)}$[HD_2]. Expressions for the individual average coupling constants are $J_{HD(obs)}$[H_2D] = $^1J_{HD}K/(1 + 2K)$ and $J_{HD(obs)}$[HD_2] = $^1J_{HD}/(2 + K)$.

(55) The initial product obtained upon elimination of H_2 is spectroscopically characterized as {[$Me_2Si(C_5Me_4)_2$]Mo(H)(L)}$^+$ (L = CD_3CN). This complex undergoes subsequent β-hydride insertion into the C≡N bond of the coordinated nitrile and, in the presence of excess acid, is protonated to form an η^1-imine complex, {[$Me_2Si(C_5Me_4)_2$]Mo[η^1-N(H)C(H)Me)(NCMe)]}$^{2+}$.

(56) [Cp_2MoH_3]$^+$ and [(Cp^{But})$_2$$MoH_3$]$^+$ also exhibit reasonable thermal stability with respect to reductive elimination.

(57) Shin, J. H.; Parkin, G. *J. Chem. Soc., Chem. Commun.* **1999**, 887−888.

(58) (a) Green, J. C.; Jardine, C. N. *J. Chem. Soc., Dalton Trans.* **1998**, 1057−1061. (b) Green, J. C.; Harvey, J. N.; Poli, R. *J. Chem. Soc., Dalton Trans.* **2002**, 1861−1866. (c) Su, M.-D.; Chu, S.-Y. *J. Phys. Chem. A* **2001**, *105*, 3591−3597.

Scheme 4

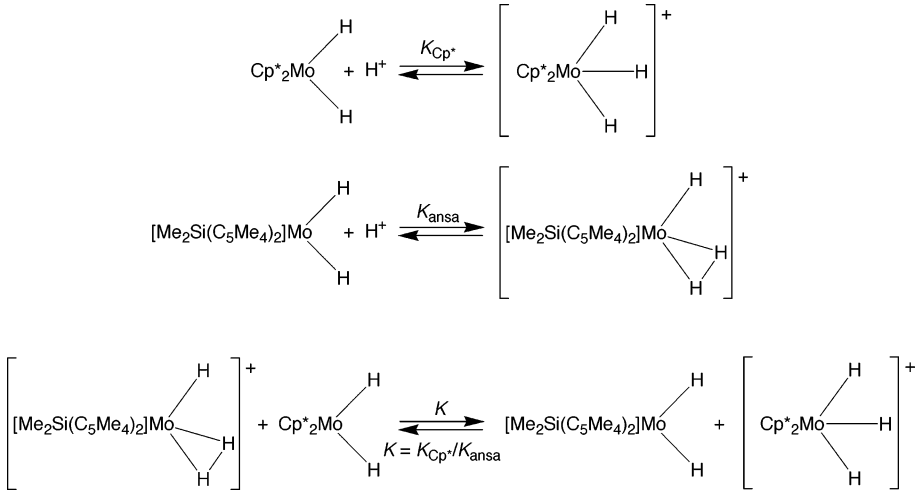

concerned with its impact on the basicity of the molybdenocene dihydride complex (Scheme 4). In this regard, a clear indication that the *ansa* bridge reduces the basicity is provided by the observation that the *ansa* complex $\{[Me_2Si(C_5Me_4)_2]Mo(\eta^2\text{-}H_2)(H)\}^+$ is readily deprotonated by $Cp^*_2MoH_2$ to give $[Me_2Si(C_5Me_4)_2]MoH_2$ and $[Cp^*_2Mo(H)_3]^+$, with an equilibrium constant $K = K_{Cp^*}/K_{ansa}$. Since the equilibrium lies heavily in favor of $[Me_2Si(C_5Me_4)_2]MoH_2$ and $[Cp^*_2Mo(H)_3]^+$, it is only possible to determine a lower limit for *K*, which is estimated to be >2500 at −30 °C, corresponding to $\Delta G < -3.8$ kcal mol^{-1}. Support for this observation is provided by theoretical calculations which indicate that deprotonation of $\{[Me_2Si(C_5Me_4)_2]Mo(\eta^2\text{-}H_2)(H)\}^+$ by $Cp^*_2MoH_2$ is exothermic by 6.09 kcal mol^{-1} in the gas phase.

It is appropriate to comment on the fact that protonation of $Cp^*_2MoH_2$ occurs thermodynamically at the metal center to yield a trihydride $[Cp^*_2Mo(H)_3]^+$, whereas protonation of $[Me_2Si(C_5Me_4)_2]MoH_2$ occurs thermodynamically at the metal−hydrogen bond to give the dihydrogen−hydride complex $\{[Me_2Si(C_5Me_4)_2]Mo(\eta^2\text{-}H_2)(H)\}^+$.[60] Thus, since $\{[Me_2Si(C_5Me_4)_2]Mo(H)_3\}^+$ is less stable (i.e. more acidic) than $\{[Me_2Si(C_5Me_4)_2]Mo(\eta^2\text{-}H_2)(H)\}^+$,[61] it is evident that the [Me$_2$Si] *ansa* bridge reduces the basicity of the metal center to an even greater degree than that indicated by the value of *K* for deprotonation of $\{[Me_2Si(C_5Me_4)_2]Mo(\eta^2\text{-}H_2)(H)\}^+$ by $Cp^*_2MoH_2$.

Computational Analysis of the Energetics Pertaining to the Interconversion of Dihydrogen−Hydride and Trihydride Isomers. A series of DFT calculations has been performed to provide more information concerned with the influence of the *ansa* bridge on the relative stability of classical trihydride and nonclassical dihydrogen−hydride isomers for $[Cp^*_2MoH_3]^+$ and $\{[Me_2Si(C_5Me_4)_2]MoH_3\}^+$. Geometry-optimized structures of the relevant species, namely $[Cp^*_2Mo(H)_3]^+$, $[Cp^*_2Mo(\eta^2\text{-}H_2)(H)]^+$, $\{[Me_2Si(C_5Me_4)_2]Mo(H)_3\}^+$, and $\{[Me_2Si(C_5Me_4)_2]Mo(\eta^2\text{-}H_2)(H)\}^+$, are illustrated in Figure 12 (selected bond lengths and energies are listed in Tables S1 and S2 of the Supporting Information). A comparison of the energy surface for the various transformations pertaining to isomerization, reductive elimination, and deprotonation of $\{[Me_2Si(C_5Me_4)_2]Mo(\eta^2\text{-}H_2)(H)\}^+$ and $[Cp^*_2MoH_3]^+$ is provided in Figures 9 and 10.

In accord with the experimental observations, the calculations indicate that the trihydride is the more stable form for $[Cp^*_2MoH_3]^+$ (by 1.5 kcal mol^{-1}), whereas the dihydrogen−hydride form is the more stable form for $\{[Me_2Si(C_5Me_4)_2]MoH_3\}^+$ (by 0.1 kcal mol^{-1}), although the difference is sufficiently small that the relative stability of the two isomers cannot be accurately assessed. Furthermore, we have performed calculations on the isomers of $[Cp_2MoH_3]^+$, $\{[H_2Si(C_5H_4)_2]MoH_3\}^+$, and $\{[Me_2Si(C_5H_4)_2]MoH_3\}^+$ which also indicate that the trihydride isomer is more stable for $[Cp_2MoH_3]^+$ whereas the dihydrogen−hydride isomers are more stable form for the *ansa* systems $\{[H_2Si(C_5H_4)_2]MoH_3\}^+$ and $\{[Me_2Si(C_5H_4)_2]MoH_3\}^+$ (Table 5). However, for each of the $[Cp^R_2MoH_3]^+$ systems studied, the preference for one isomer over the other is not strong (<3 kcal mol^{-1}).[19] In this regard, it is pertinent to note that the *ansa* tungstenocene system $\{[Me_2C(C_5H_4)_2]WH_3\}^+$ also exhibits a small difference in stability (1.7 kcal mol^{-1}), but it is the trihydride that is calculated to be the more stable,[14a] in line with the observation that metals of the third transition series more commonly yield classical hydride complexes than do their second transition series congeners.[3] The comparable energies of the dihydrogen−hydride and trihydride isomers in these systems indicates that small variations in ligand substituents can cause the ground state to shift between isomers.

In addition to assessing the relative stabilities of trihydride and dihydrogen−hydride isomers by DFT calculations, we have also probed the two fluxional processes that have been observed

(59) For related *ansa* effects pertaining to olefin insertion in $(Cp^R)_2M(C_2H_4)H$ (M = Nb, Ta), see: Ackerman, L. J.; Green, M. L. H.; Green, J. C.; Bercaw, J. E. *Organometallics* **2003**, *22*, 188−194.

(60) It should be emphasized that this statement is not intended to comment on the issue of whether protonation at the metal or the metal−hydride bond is kinetically favored or not. However, a variety of investigations suggest that protonation at the metal−hydride bond is more facile than direct protonation at the metal center. See, for example: (a) Papish, E. T.; Rix, F. C.; Spetseris, N.; Norton, J. R.; Williams, R. D. *J. Am. Chem. Soc.* **2000**, *122*, 12235−12242. (b) Belkova, N. V.; Revin, P. O.; Epstein, L. M.; Vorontsov, E. V.; Bakhmutov, V. I.; Shubina, E. S.; Collange, E.; Poli, R. *J. Am. Chem. Soc.* **2003**, *125*, 11106−11115. (c) Belkova, N. V.; Gutsul, E. I.; Shubina, E. S.; Epstein L. M. *Z. Phys. Chem.* **2003**, *217*, 1525−1538. (d) References 9 and 16.

(61) Whereas the *ansa* trihydride $\{[Me_2Si(C_5Me_4)_2]Mo(H)_3\}^+$ is more acidic than its dihydrogen−hydride tautomer $\{[Me_2Si(C_5Me_4)_2]Mo(\eta^2\text{-}H_2)(H)\}^+$, the reverse is true for the non-*ansa* system, for which the dihydrogen−hydride complex $[Cp^*_2Mo(\eta^2\text{-}H_2)(H)]^+$ is more acidic than the trihydride $[Cp^*_2Mo(H)_3]^+$. It is manifest that this is merely a reflection of the differing stabilities of dihydrogen−hydride versus trihydride isomers for the two systems.

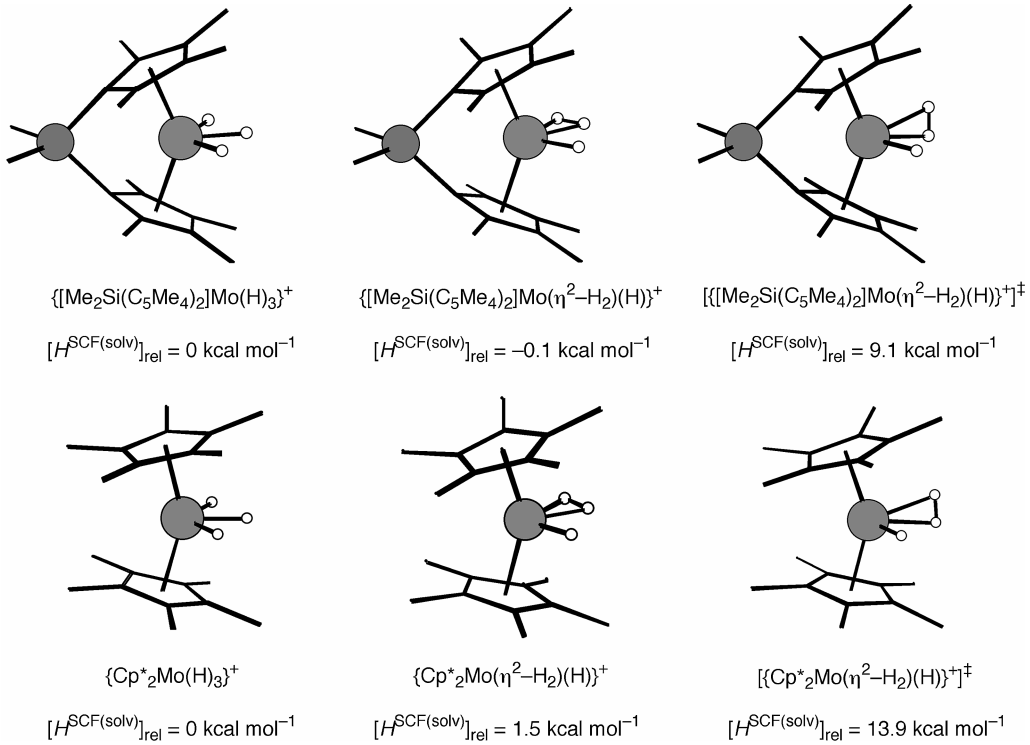

Figure 12. Geometry-optimized structures of the trihydride and dihydrogen−hydride isomers, together with the transition state for rotation of the dihydrogen ligand for $\{[Me_2Si(C_5Me_4)_2]MoH_3)\}^+$ and $[Cp^*_2MoH_3]^+$ systems.

Table 5. Calculated Enthalpies of $\{(Cp^R)_2Mo(\eta^2\text{-}H_2)(H)\}^+$ Relative to Those of the $\{(Cp^R)_2Mo(H)_3\}^+$ Isomers

	$H^{SCF}\{Mo(\eta^2\text{-}H_2)(H)\} - H^{SCF}\{Mo(H)_3\}$	
	$\Delta H^{SCF(g)}$/ kcal mol^{-1}	$\Delta H^{SCF(solv)}$/ kcal mol^{-1}
$\{[Me_2Si(C_5Me_4)_2]MoH_3\}^+$	0.2	−0.1
$\{[Me_2Si(C_5H_4)_2]MoH_3\}^+$	−1.4	−0.9
$\{[H_2Si(C_5H_4)_2]MoH_3\}^+$	−1.5	−1.0
$[Cp_2MoH_3]^+$	1.8	2.9
$[Cp^*_2MoH_3]^+$	2.0	1.5

by ^{1}H NMR spectroscopy, namely (i) the facile "side-to-side" motion of the central hydrogen which is rapid on the NMR time scale at all temperatures studied, and (ii) the slower rotation of the dihydrogen unit that may be frozen on the NMR time scale. As would be expected, the barrier for "side-to-side" motion of the central hydrogen atom converting the dihydrogen−hydride isomer to the trihydride is low, and is calculated to be 2.4 kcal mol^{-1} for $\{[Me_2Si(C_5Me_4)_2]Mo(\eta^2\text{-}H_2)(H)\}^+$.[62]

By comparison to the facile "side-to-side" motion, the barrier to rotation of the dihydrogen ligand is sufficiently large that it may be frozen on the NMR time scale. Calculations confirm this observation, with the computed transition state for dihydrogen rotation within $\{[Me_2Si(C_5Me_4)_2]Mo(\eta^2\text{-}H_2)(H)\}^+$ being 9.2 kcal mol^{-1} above that of the ground state; for comparison, the experimental $\Delta H^‡$ for rotation of the dihydrogen ligand is 10.2 kcal mol^{-1}. The geometry of the transition state is one in which the dihydrogen ligand is almost perpendicular to the metallocene plane (Figure 12).[14a,27] Other noteworthy features of the $[Mo(H_2)]$ moiety at the transition state are that the H−H distance is shorter than in the ground state (0.77 versus 0.90 Å) while the average Mo−H distance is longer (1.90 versus 1.79 Å); the shorter H−H distance in the transition state for dihydrogen rotation is consistent with the notion of reduced back-bonding in this orientation.[14a]

The computed barrier to site exchange of the central and lateral hydrogen atoms of the non-*ansa* system via a $\{[Cp^*_2Mo(\eta^2\text{-}H_2)(H)]^{+\,‡}$ transition state is 13.9 kcal mol^{-1} relative to $[Cp^*_2Mo(H)_3]^+$. Thus, the $[Me_2Si]$ *ansa* bridge is calculated to have a significant impact on the barrier to rotation of the dihydrogen ligand. These results are also in accord with the experimental study of central/lateral hydride exchange which indicates that the enthalpy barrier for $\{[Me_2Si(C_5Me_4)_2]Mo(\eta^2\text{-}H_2)(H)\}^+$ ($\Delta H^‡ = 10.2$ kcal mol^{-1}) is ca. 7 kcal mol^{-1} lower than that for $[Cp^*_2Mo(H)_3]^+$ ($\Delta H^‡ = 17.0$ kcal mol^{-1}).

Experimental Section

General Considerations. Unless otherwise noted, all reactions and manipulations were performed under an Ar or N_2 atmosphere employing standard Schlenk and glovebox techniques. Solvents were dried by passing through activated alumina prior to use using a system purchased from Glass Contour (Laguna Beach, CA). Acetone-d_6 and acetonitrile-d_3 were purchased from Cambridge Isotopes and used as received. All spectra were collected on either a Bruker 300wb DRX or a Bruker Advance 500 DMX spectrometer. ^{1}H and ^{13}C chemical shifts are reported in ppm relative to $SiMe_4$ ($\delta = 0$) and were referenced internally with respect to the residual protio impurity ($\delta = 2.04$ for acetone and $\delta = 1.93$ for acetonitrile) and the ^{13}C resonances of the solvent ($\delta =$

(62) A reviewer has suggested that it is possible to calculate an upper limit for $\Delta G^‡$ for "side-to-side" exchange on the basis of the observed data. However, since the chemical shifts of the hydride and *exo* hydrogen of the dihydrogen ligand are not known, but only their average, it is not possible to determine an upper limit for $\Delta G^‡$ unless an assumption is made regarding the chemical shift of one of these sites. While it could be reasonable to assume that the two hydrogen atoms of the dihydrogen ligand would have similar chemical shifts, Chaudret (ref 39) has demonstrated that they may differ by more than 1 ppm. Nevertheless, with this caveat, an upper limit of 5.3 kcal mol^{-1} may be estimated for $\Delta G^‡$ for "side-to-side" exchange if it is assumed that the two hydrogen atoms of the dihydrogen ligand have the same chemical shifts.

1.30 ppm for CD_3CN). Cp_2MoH_2,[63] $(Cp^{But})_2MoH_2$,[18a] $Cp^*_2MoH_2$,[18b] $[Me_2Si(C_5Me_4)_2]MoH_2$,[18c] and $[Cp_2MoH_3][BF_4]$[8] were prepared according to literature methods. NMR simulations were performed using g-NMR.

Synthesis of $[Cp^*_2MoH_3][BF_4]$ and $[(Cp^{But})_2MoH_3][BF_4]$. A stirred solution of $Cp^*_2MoH_2$ (200 mg, 0.54 mmol) in Et_2O (30 mL) at −78 °C was treated dropwise with a solution of HBF_4 in Et_2O (50% w/w, 300 μL), resulting in the deposition of a light gray precipitate. The mixture was stirred at −78 °C for 10 min and then allowed to warm to 0 °C and stirred at this temperature for 30 min. The light gray precpitate was allowed to settle and the mixture was filtered. The residue was washed with Et_2O (3 × 10 mL) and dried in vacuo, yielding $[Cp^*_2MoH_3][BF_4]$ as a light gray powder (110 mg, 45% yield). ^{1}H NMR (CD_3CN; 25 °C): −5.51 ppm [s, 3H, Mo*H*], 1.99 ppm [s, 30H, C_5Me_5]. ^{13}C NMR (CD_3CN; 25 °C): 11.33 ppm [q, $^1J_{C-H}$ = 130 Hz, C_5Me_5], 105.13 ppm [s, C_5Me_5]. A mixture of $[Cp^*_2MoH_xD_{(3-x)}]^+$ isotopologues was obtained by addition of MeOH-d_4 (50 μL) to a solution of $[Cp^*_2MoH_3][BF_4]$ in Me_2CO-d_6 at room temperature. $[(Cp^{But})_2MoH_3][BF_4]$ was prepared in an analogous manner.

Synthesis of $\{[Me_2Si(C_5Me_4)_2]MoH_3\}[A]$ ($A^- = [BAr^f_4]^-$ or $[BF_4]^-$). A solution of $[Me_2Si(C_5Me_4)_2]MoH_2$ (4 mg, 0.010 mmol) in Me_2CO-d_6 (500 μL) in a 5 mm J. Young NMR tube was cooled to −78 °C and treated with a solution of $[H(OEt_2)_2][BAr^f_4]$ (25 mg, 0.025 mmol) in Me_2CO-d_6 (200 μL) (Ar^f = 3,5-bis(trifluoromethyl)phenyl).[64] The NMR tube was placed in a precooled NMR probe, thereby demonstrating the formation of $\{[Me_2Si(C_5Me_4)_2]MoH_3\}[BAr^f_4]$ (see text). $\{[Me_2Si(C_5Me_4)_2]MoH_3\}[BF_4]$ was obtained in an analogous manner using a solution of HBF_4 in Et_2O (50% w/w) in Me_2CO-d_6. A mixture of $\{[Me_2Si(C_5Me_4)_2]MoH_xD_{(3-x)}\}^+$ isotopologues was obtained by the use of $[D(OEt_2)_2][BAr^f_4]$ and by allowing H/D exchange with Me_2CO-d_6.

Kinetics of Dihydrogen Elimination from $[Cp^*_2MoH_3][BF_4]$ and $\{[Me_2Si(C_5Me_4)_2]MoH_3\}[BF_4]$. The kinetics of elimination at 20 °C was monitored by ^{1}H NMR spectroscopy using CD_3CN as solvent in order to prevent H/D exchange between hydride and solvent. Since the elimination of H_2 from $\{[Me_2Si(C_5Me_4)_2]MoH_3\}^+$ is rapid, the sample was allowed to thaw in the precalibrated (20 °C) NMR probe and spectra were acquired at specified intervals. The kinetics of elimination for both compounds showed first-order loss of dihydrogen over 3 half-lives.

Computational Details. All calculations were carried out using DFT as implemented in the Jaguar 4.1 suite of ab initio quantum chemistry programs.[65] Geometry optimizations and frequency calculations were performed with the B3LYP functional and the 6-31G** (C, H, Si) and LACVP** (Mo) basis sets. The energies of the optimized structures were reevaluated by additional single-point calculations on each optimized geometry using the cc-pVTZ(-f) (C, H, Si) and LACV3P** (Mo) basis sets. Solvation energies were calculated for the 6-31G** and LACVP** basis sets using the Jaguar Poisson−Boltzmann solver, with the dielectric constant set to a value of 20.7 for acetone. Vibrational frequency calculations were performed at the B3LYP level of theory using 6-31G** and LACVP** basis sets. Cartesian coordinates for the derived geometries and vibrational frequencies are listed in the Supporting Information.

Conclusions

In summary, experimental and computational studies on a series of cationic molybdenocene trihydride complexes, namely $[Cp_2MoH_3]^+$, $[(Cp^{But})_2MoH_3]^+$, $[Cp^*_2MoH_3]^+$, and $\{[Me_2Si(C_5Me_4)_2]MoH_3\}^+$, demonstrate that the most stable form for the *ansa* molybdenocene derivative is a nonclassical dihydrogen−hydride isomer, $\{[Me_2Si(C_5Me_4)_2]Mo(\eta^2\text{-}H_2)(H)\}^+$, whereas the stable forms for the non-*ansa* complexes are classical trihydrides, $[Cp_2Mo(H)_3]^+$, $[(Cp^{But})_2Mo(H)_3]^+$, and $[Cp^*_2Mo(H)_3]^+$. For example, at −80 °C, the T_1 relaxation time of $\{[Me_2Si(C_5Me_4)_2]MoH_3\}^+$ (33 ms) is almost an order of magnitude shorter than that for $[Cp^*_2MoH_3]^+$ (291 ms), consistent with a short H···H separation in the former compound. Furthermore, while $[Cp^*_2MoH_2D]^+$ and $[Cp^*_2MoHD_2]^+$ exhibit neither isotopic perturbation of chemical shift nor J_{HD} coupling at room temperature, the corresponding isotopologues of the *ansa* system, $\{[Me_2Si(C_5Me_4)_2]MoH_2D\}^+$ and $\{[Me_2Si(C_5Me_4)_2]MoHD_2\}^+$, exhibit both isotopic perturbation of chemical shift and resolvable J_{HD} coupling, consistent with a dihydrogen−hydride formulation. Low-temperature studies enable $^1J_{HD}$ for $\{[Me_2Si(C_5Me_4)_2]Mo(\eta^2\text{-}HD)(H)\}^+$ (26.8 Hz) and $\{[Me_2Si(C_5Me_4)_2]Mo(\eta^2\text{-}HD)(D)\}^+$ (26.4 Hz) to be determined, from which the H−H distance is estimated to be 0.98 Å by application of the empirical bond length/coupling constant correlation.

Although the hydride ligands of $\{[Me_2Si(C_5Me_4)_2]Mo(\eta^2\text{-}H_2)(H)\}^+$ are characterized by a singlet at the lowest temperature studied (−95 °C), studies on the isotopologues $\{[Me_2Si(C_5Me_4)_2]MoH_2D\}^+$ and $\{[Me_2Si(C_5Me_4)_2]MoHD_2\}^+$ provide evidence for the hindered rotation of the η^2-HD ligand; "side-to-side" motion of the central hydrogen or deuterium atom, however, remains rapid on the NMR time scale at all temperatures studied. The principal reason why hindered rotation may not be observed for the η^2-H_2 ligand is a consequence of a large J_{HH} coupling constant and rapid "side-to-side" motion of the central hydrogen, the combination of which causes the highly second-order ABC spectrum to collapse to a singlet. The barrier to rotation of the dihydrogen ligand in $\{[Me_2Si(C_5Me_4)_2]Mo(\eta^2\text{-}HD)(H)\}^+$ ($\Delta G^{\ddagger}_{25°C}$ = 9.0 kcal mol^{-1}) is substantially smaller than the barrier to central/lateral site exchange of the hydride ligands in $[Cp^*_2MoH_3]^+$ ($\Delta G^{\ddagger}_{25°C}$ = 14.3 kcal mol^{-1}), corresponding to a factor of ∼8000 in rate constant.

The preference of deuterium relative to hydrogen to occupy hydride versus dihydrogen sites within the isotopologues $\{[Me_2Si(C_5Me_4)_2]MoH_2D\}^+$ and $\{[Me_2Si(C_5Me_4)_2]MoHD_2\}^+$ has been addressed by using computational methods on a simpler system in which the methyl groups of the $[Me_2Si(C_5Me_4)_2]$ ligand are replaced by hydrogen atoms, i.e. isotopomers of $\{[H_2Si(C_5H_4)_2]MoH_2D\}^+$ and $\{[H_2Si(C_5H_4)_2]MoHD_2\}^+$. These studies establish that deuterium exhibits a greater preference than hydrogen to occupy dihydrogen sites in this system.

In addition to altering the classical versus nonclassical nature of $[Cp^*_2MoH_3]^+$ and $\{[Me_2Si(C_5Me_4)_2]Mo(\eta^2\text{-}H_2)(H)\}^+$, the $[Me_2Si]$ *ansa* bridge also influences the stability of the complex with respect to elimination of H_2 and dissociation of H^+. Thus, (i) elimination of H_2 from $\{[Me_2Si(C_5Me_4)_2]Mo(\eta^2\text{-}H_2)(H)\}^+$ is more facile by a factor of ∼300 in rate constant than that of $[Cp^*_2MoH_3]^+$, and (ii) the acidity of $\{[Me_2Si(C_5Me_4)_2]Mo(\eta^2\text{-}H_2)(H)\}^+$ is greater than that of $[Cp^*_2MoH_3]^+$, as evidenced by the fact that $\{[Me_2Si(C_5Me_4)_2]Mo(\eta^2\text{-}H_2)(H)\}^+$ is readily deprotonated by $Cp^*_2MoH_2$. In each case, the ability of the $[Me_2Si]$ *ansa* bridge to (i) favor a dihydrogen−hydride isomer, (ii) promote elimination of H_2, and (iii) increase the acidity of $\{[Me_2Si(C_5Me_4)_2]Mo(\eta^2\text{-}H_2)(H)\}^+$ relative to $[Cp^*_2MoH_3]^+$ may be rationalized by the *ansa* ligand being overall less electron-donating than two cyclopentadienyl ligands.

(63) Green, M. L. H.; Knowles, P. J. *J. Chem. Soc., Perkin Trans. 1* **1973**, 989−991.
(64) Brookhart, M.; Grant, B.; Volpe, A. F., Jr. *Organometallics* **1992**, *11*, 3920−3922.
(65) Jaguar 4.1, Schrödinger, Inc., Portland, OR, 2001.

Acknowledgment. We thank the U.S. Department of Energy, Office of Basic Energy Sciences (DE-FG02-93ER14339), for support of this research and Professor Bruno Chaudret for valuable discussions. The reviewers of this manuscript are thanked for very helpful comments, and Professor D. M. Heinekey is thanked for a preprint of ref 19.

Supporting Information Available: Additional spectroscopic data; Eyring plot for rotation of the HD ligand in $\{[Me_2Si(C_5Me_4)_2]Mo(\eta^2\text{-HD})(H)\}^+$; computational details for calculation of the relative preferences of hydrogen and deuterium to occupy the classical versus nonclassical sites in $\{[Me_2Si(C_5Me_4)_2]MoH_2D\}^+$ and $\{[Me_2Si(C_5Me_4)_2]MoHD_2\}^+$; Cartesian coordinates and vibrational frequencies for geometry optimized structures. This material is available free of charge via the Internet at http://pubs.acs.org.

JA047554C